ORNL-TM-4272

HOME

HELP

COMPATIBILITY OF BRAZING ALLOYS AND THE MOLTEN SALT $NaBF_4$—8 MOLE PERCENT NaF AT 610°C

J. W. Koger

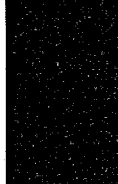

OAK RIDGE NATIONAL LABORATORY

OPERATED BY UNION CARBIDE CORPORATION • FOR THE U.S. ATOMIC ENERGY COMMISSION

ORNL-TM-4272

Contract No. W-7405-eng-26

METALS AND CERAMICS DIVISION

COMPATIBILITY OF BRAZING ALLOYS AND THE MOLTEN SALT $NaBF_4$–8 MOLE PERCENT NaF AT 610°C

J. W. Koger

December 1972

OAK RIDGE NATIONAL LABORATORY
Oak Ridge, Tennessee 37830
operated by
UNION CARBIDE CORPORATION
for the
U.S. ATOMIC ENERGY COMMISSION

CONTENTS

COMPATIBILITY OF BRAZING ALLOYS AND THE MOLTEN SALT $NaBF_4$–8 MOLE PERCENT NaF AT 610°C

J. W. Koger

ABSTRACT

A comprehensive review of the compatibility of braze alloys with molten fluoride salts was performed. Eight different braze alloys, used to braze Hastelloy N, were exposed to $NaBF_4$–8 mole % NaF at 610°C for 4987 hr. On the basis of weight changes, microstructural changes, and electron microprobe analysis all alloys tested were compatible. The Ag–28% Cu and 100% Cu braze alloys were considered the most resistant. The prediction of corrosion resistance on the basis of free energy of formation data was in reasonable agreement with our results. Nickel transferred to non-nickel-containing braze alloys through an activity gradient mass transfer mechanism. Some deposits were noted on the Hastelloy N base material. Significant interdiffusion of the Hastelloy N and the braze alloy occurred only with those braze alloys whose composition was near that of Hastelloy N.

1. INTRODUCTION

The most recent designs for the molten-salt breeder reactor (MSBR) call for two salts: one containing both fertile and fissile material (ThF_4 and UF_4) and one that will transfer heat from this fuel salt to a steam generator. The tentative choice for this latter salt is the eutectic sodium fluoroborate–sodium fluoride mixture $NaBF_4$–8 mole % NaF, chosen because of its low melting point, low cost, and acceptable heat-transfer properties. Until recently, little was known about the compatibility of this salt with alloys considered for use in a molten salt reactor system. The nickel-based Hastelloy N alloy has been tentatively chosen for use in molten fluoride salts, and many tests have been conducted on its compatibility with the sodium fluoroborate mixture.[1–11]

Welded and back-brazed tube-to-tube-sheet joints are normally used in the fabrication of heat exchangers for molten-salt service. The back-brazing operation serves to remove the notch inherent in conventional tube-to-tube-sheet joints, and the braze material minimizes the possibility of leakage through a weld failure that might be created by thermal stresses in service. Thus the braze material must be resistant to corrosion caused by the molten salt. Also, as larger engineering loops are built, other uses for brazes that will contact the sodium fluoroborate mixture will surely be found. However, no tests have been conducted to establish the compatibility of braze alloys (specifically those that could be used with Hastelloy N) with $NaBF_4$–8 mole % NaF. This report details an experiment conducted to determine the compatibility of various Hastelloy N braze alloys with the sodium fluoroborate mixture at 610°C, the maximum

---

1. J. W. Koger and A. P. Litman, *MSR Program Semiannu. Progr. Rep. Feb. 29, 1968,* ORNL-4254, pp. 218–25.
2. J. W. Koger and A. P. Litman, *MSR Program Semiannu. Progr. Rep. Aug. 31, 1968,* ORNL-4344, pp. 257–66.
3. J. W. Koger and A. P. Litman, *MSR Program Semiannu. Progr. Rep. Feb. 28, 1969,* ORNL-4396, pp. 243–53.
4. J. W. Koger and A. P. Litman, *MSR Program Semiannu. Progr. Rep. Aug. 31, 1969,* ORNL-4449, pp. 195–208.
5. J. W. Koger, *MSR Program Semiannu. Progr. Rep. Feb. 28, 1970,* ORNL-4548, pp. 240–52.
6. J. W. Koger, *MSR Program Semiannu. Progr. Rep. Aug. 31, 1970,* ORNL-4622, pp. 165–78.
7. J. W. Koger, *MSR Program Semiannu. Progr. Rep. Feb. 28, 1971,* ORNL-4676, pp. 192–215.
8. J. W. Koger and A. P. Litman, *Compatibility of Hastelloy N and Croloy 9M with $NaBF_4$-NaF-KBF_4 (90-4-6 mole %) Fluoroborate Salt,* ORNL-TM-2490 (April 1969).
9. H. E. McCoy, R. L. Beatty, W. H. Cook, R. E. Gehlbach, C. R. Kennedy, J. W. Koger, A. P. Litman, C. E. Sessions, and J. R. Weir, "New Developments in Materials for Molten Salt Reactors," *Nucl. Appl. Technol.*, 8, 156 (1970).
10. J. W. Koger and A. P. Litman, *Compatibility of Fused Sodium Fluoroborates and BF_3 Gas with Hastelloy N Alloys,* ORNL-TM-2978 (June 1970).
11. J. W. Koger and A. P. Litman, *Mass Transfer Between Hastelloy N and Haynes Alloy No. 25 in a Molten Sodium Fluoroborate Mixture,* ORNL-TM-3488 (October 1971).

Table 1. Braze alloys, brazing temperature, and composition

No.	AWS-ASTM classification	Brazing temperature (°C)	Composition (wt %)									
			Cr	Fe	Ni	P	C	Si	B	Au	Cu	Ag
1	BNi-7	1010	13		76.85	10	0.15					
2	BNi-3	1040		3.5	89.1			4.5	2.9			
3	BAu-4	1010			18					82		
4	BAg-8	816									28	72
5	BNi-4	1040			92.35		0.15	4.5	3			
6	BCu	1125									100	
7	BNi-2[a]	1030	7	3.5	82.1			4.5	2.9			
8	BNi-2[a]	1040	6.5	2.5	83.35		0.15	4.5	3			

[a]Two different manufacturers.

temperature proposed for the salt use. Eight fairly typical brazes were selected for this experiment. The braze alloys, their composition, and the temperature of brazing are listed in Table 1.

2. PREVIOUS WORK

Many experiments have been previously conducted to determine which braze alloys (suitable for use with nickel alloys) would be acceptable in a high-temperature molten-salt environment containing UF_4. Some of these results will be reviewed in order to compare like-brazing alloys in different fluoride salt experiments, keeping in mind temperature, time, and test differences.

Brazing alloys of composition 91.25% Ni–4.5% Si–2.9% B (quite similar to the BNi-4 we tested) and 93.25% Ni–3.5% Si–1.9% B in button form were subjected to 100-hr corrosion tests in the fuel mixture NaF–40.0 mole % ZrF_4–6.5 mole % UF_4 in a seesaw apparatus (a rocking furnace combined with a temperature gradient, described by Vreeland et al.[12]) at a hot-zone temperature of 816°C.[13] Minor constituents of the alloys were leached to a depth of 1 to 2 mils, as shown by metallography, and weight losses of the alloy specimens varied from 0.03 to 0.06%.

The brazing alloys Au–18% Ni (which we tested, BAu-4) and Au–20% Cu were corrosion tested in LiF–41.0 mole % KF–11.2 mole % NaF–2.5 mole % UF_4 and LiF–37.0 mole % BeF_2–1.0 mole % UF_4 for 2000 hr at 650°C under static conditions.[14] The alloys were also tested in the latter fuel for 500 hr in a seesaw apparatus with a hot-zone temperature of 650°C. No attack was observed on either alloy in any of the tests. A layer high in nickel was found on the Au–18% Ni specimen after tests in both salts.

Four silver-base brazing materials, ranging in composition from pure silver to alloys with 42 wt % silver, and a gold-base alloy (Au–20% Cu–5% Ag) were tested in static LiF–37.0 mole % BeF_2–1.0 mole % UF_4 at 700°C for 500 hr.[15] As shown in Table 2, subsurface voids, as deep as 50 mils in the case of pure silver, were observed in all the silver-containing alloys. The gold-based alloy showed no corrosion.

In order to obtain long-term dynamic corrosion data on brazing alloys in LiF–37.0 mole % BeF_2–1 mole % UF_4, a series of five alloys were tested in duplicate by inserting brazed lap joints (nickel-base alloys, similar configuration to that which we used) in the hot legs of thermal-convection loops.[16] (We tested all

12. D. C. Vreeland, E. E. Hoffman, and W. D. Manly, *Nucleonics* 11(11), 36–39 (1953).
13. D. H. Jansen, *ANP Quart. Progr. Rep. Dec. 31, 1957,* ORNL-2440, p. 169.
14. D. H. Jansen, *MSR Quart. Progr. Rep. Jan. 31, 1958,* ORNL-2474, p. 59.
15. D. H. Jansen, *MSR Quart. Progr. Rep. Oct. 31, 1958,* ORNL-2626, p. 64.
16. E. E. Hoffman and D. H. Jansen, *MSR Quart. Progr. Rep. June 30, 1958,* ORNL-2551, p. 62.

Table 2. Results of corrosion tests of silver- and gold-base brazing alloys exposed to static LiF–37.0 mole % BeF_2–1.0 mole % UF_4 for 500 hr at 700°C

Braze material	Metallographic results
Pure silver	Spotty, heavy attack; stringers to a depth of 50 mils in some places
Ag–10% Cu	Rather uniform, heavy attack to a depth of 16 mils
Ag–33.3% Au–16.7% Cu	Spotty attack to a maximum depth of 5 mils
Ag–40% Au–18% Cu–0.6% Zn	Uniform attack to a depth of 15 mils
Au–20% Cu–5% Ag	No attack

Table 3. Results of metallographic examinations of brazing materials tested in thermal-convection loop circulating LiF–37 mole % BeF_2–1 mole % UF_4

Test conditions: hot-leg temperature, 700°C; cold-leg temperature, 593°C

AWS-ASTM classification	Alloy composition (%)	Time (hr)	Metallographic results: alloy brazed to –	
			Inconel	Hastelloy N
BNi-3	89 Ni–5 Si–4 B–2 Fe	5,000	No attack	No attack
		10,000	Diffusion voids to 3 mils below surface	No attack
BNi-2	81 Ni–8 Cr–4 B–4 Si–3 Fe	5,000	No attack	No attack
		10,000	Severe porosity 15 mils deep	No attack
BNi-5	70 Ni–20 Cr–10 Si	5,000	Heavy attack of 16 mils	3 mil attack
		10,000	Complete attack; severe porosity through fillet	No attack
BAu-4	82 Au–18 Ni	5,000	No attack	No attack
		10,000	No attack	No attack
BCu	100 Cu	5,000	No attack; diffusion voids 2 mils deep on fillet	No attack; diffusion voids 2 mils deep
		10,000	No attack; small diffusion voids present in fillet	No attack

but the BNi-5 alloy.) A series of three identical loops were operated for 1,000, 5,000, and 10,000 hr with the temperature of the circulating salt in the region of the test specimens at 700°C.

Metallographic examination after the 1000-hr test showed that all the brazing alloys had good flowability on both Inconel and Hastelloy N.[17] There was a tendency for the formation of diffusion voids in the fillets of the joints brazed with the gold-nickel alloy. The BNi-5 alloy was heavily attacked on Inconel. The BNi-3 and BNi-2 were depleted at the fillet surface to a depth of 1 to 2 mils. Some slight cracking of the alloys occurred at the brazing-alloy–base-metal interface. Pure copper showed good corrosion resistance and no cracking.

The results of the 5000- and 10,000-hr tests are outlined in Table 3 (refs. 18 and 19). Copper, gold-nickel, and the BNi-3 and BNi-2 alloys showed good corrosion resistance after 5000 hr. A depleted

17. *MSR Quart. Progr. Rep. April 30, 1959,* ORNL-2723, pp. 60–61.
18. *MSR Quart. Progr. Rep. Oct. 31, 1959,* ORNL-2890, pp. 46–47.
19. *MSR Quart. Progr. Rep. Jan. 31 and April 30, 1960,* ORNL-2973, pp. 62–63.

Table 4. Results of static corrosion tests on refractory-metal-base brazing alloys in LiF–37 mole % BeF_2–1 mole % UF_4 in nickel containers

Test conditions: time, 100 hr; temperature, 700°C

Alloy composition (%)	Weight change (%)
48 Ti–48 Zr–4 Be	–4.2
95 Ti–5 Be	–6.5
95 Ti–5 Be	–9.8

Table 5. Results of static corrosion tests on refractory metals in LiF–37 mole % BeF_2–1 mole % UF_4 in containers of several materials

Test conditions: time, 100 hr; temperature, 700°C

Material	Weight change (%) when tested in –			
	Nickel	Hastelloy N	Titanium	Zirconium
Ti	–12.1	–7.6	–0.71	
Zr	–11.7	–4.2		–0.08
Be	Excessive, portion of sample dissolved			

region to a depth of 3 mils was observed along the BNi-3 and BNi-2 alloy fillets after the test. Results of earlier corrosion tests on these alloys in NaF-ZrF_4-base fuels and in liquid metals indicated that this depletion was due to the leaching of the minor constituents boron and silicon from the alloy by the bath, and it appears that boron and silicon are also being leached by the salt. This depletion has no detrimental effect on the alloy, since a nickel-rich, corrosion-resistant matrix is left.

After 10,000 hr all the brazed joints showed good corrosion resistance when used to join Hastelloy N. However, Inconel joints brazed with BNi-3, BNi-2, and BNi-5 were attacked. Thus the results from the 1,000-, 5,000-, and 10,000-hr corrosion tests indicate that several brazing materials suitable for joining Hastelloy N or Inconel have adequate corrosion resistance to the type of fluoride salt represented by LiF–37.0 mole % BeF_2–1.0 mole % UF_4.

Some refractory-metal-base alloys being developed by the Welding and Brazing Group at ORNL for possible application in joining graphite to graphite were given a static corrosion test in LiF–37.0 mole % BeF_2–1.0 mole % UF_4 for 100 hr at 700°C (ref. 20). Because of its comparative inertness to fluorides, nickel was used as the test-container material. Test results listed in Table 4 showed large weight losses for each alloy. In order to determine the alloying element or elements responsible for the heavy attack, the following static corrosion tests in LiF–37.0 mole % BeF_2–1.0 mole % UF_4 were conducted at 700°C: (1) titanium was tested in containers of titanium, nickel, and Hastelloy N; (2) zirconium was tested in containers of zirconium, nickel, and Hastelloy N; and (3) beryllium was tested in a nickel container. Large weight losses (Table 5) were observed for specimens tested in nickel or nickel-base containers, while small weight losses were found when specimen and container were of the same metal. Substituting a Hastelloy N (containing 70% Ni) container for one of pure nickel resulted in a weight-loss decrease on the titanium and

20. *MSR Quart. Progr. Rep. Oct. 31, 1959*, ORNL-2890, pp. 46–47.

Table 6. Results of fuel corrosion tests on newly developed brazing alloys

Test conditions: time, 100 hr; temperature, 700°C

Alloy composition (wt %)	Test container	Type of test specimen	Fuel used as bath[a]	Weight change (mg)	Metallographic results
60 Au–30 Ta–10 Ni	Nickel capsule	Alloy button	130	–3	Slight, scattered subsurface voids to 1 mil in depth
62 Au–26 Ta–12 Ni	Nickel capsule	Graphite-Mo T-joint	130	+36	Slight, scattered subsurface voids to 2 mils in depth
58 Au–27 Ni–8 Ta–3 Mo–2 Cr–2 Fe	Inconel capsule	Alloy button	30	–0.9	No attack observed
63 Au–29 Ni–3.5 Mo–2.5 Cr–2 Fe	Inconel capsule	Alloy button	30	NA[b]	No attack observed

[a]130: LiF–37.0 mole % BeF_2–1.0 mole % UF_4;
30: NaF–46.0 mole % ZrF_4–4.0 mole % UF_4.

[b]Not available.

zirconium specimens. Metallographic examination and spectrographic results on the nickel capsules revealed surface layers containing titanium, zirconium, or beryllium, corresponding to the major component of the brazing alloy or metal tested. Results of the tests indicate that the usefulness of titanium-, zirconium-, or beryllium-containing brazing alloys in LiF–37.0 mole % BeF_2–1.0 mole % UF_4 would be limited in systems constructed of nickel or nickel-base alloys. Work was also done by the Welding and Brazing Group at ORNL on gold-base alloys containing various amounts of tantalum, nickel, and other minor constituents to provide proper flowability and melting point.[21] The results of corrosion tests on these alloys in different fuel salts are listed in Table 6. A moderate concentration of tantalum was detected spectrographically on the inside walls of the nickel container from the Au–30% Ta–10% Ni test. This dissimilar-metal mass transfer was not intense enough to be detected on the nickel capsule by metallographic examination. The relatively large weight gain on the graphite-to-molybdenum T-joint was due to pickup of fuel by the graphite. The two alloys listed last in Table 6 showed good resistance to NaF–46.0 mole % ZrF_4–4.0 mole % UF_4.

Tables 7 and 8 summarize the data obtained from numerous other braze-alloy–salt compatibility tests.[22] Examination of these data indicates that BCu, BAu-4, 60Pd-40Ni, BNi-3, BNi-1, and BNi-7 are satisfactory for molten-salt service.

3. EXPERIMENTAL PROCEDURE

Sixteen brazed specimens (two with each braze alloy) were prepared in the lap joint configuration shown in Fig. 1. The two joined pieces of base alloy were Hastelloy N, nominal composition 16% Mo, 7% Cr, 5% Fe, bal Ni. The test was conducted on eight specimens (one specimen of each braze) in a nickel pot at 610°C for 4987 hr. At various times the specimens were removed for weight-change measurements, and salt samples were taken for analysis of impurities. The compatibility was evaluated through weight-change measurements, salt analyses, metallographic observations, and microprobe analysis.

21. *MSR Quart. Progr. Rep. Jan. 31 and April 30, 1960,* ORNL-2973, pp. 62–64.

22. H. G. MacPherson, "Molten Salt Reactors," pp. 815–16 in *Reactor Handbook, Second Edition, Volume IV Engineering,* ed. by S. McLain and J. H. Mortens, Interscience, New York, 1964.

Table 7. Brazing alloys on Inconel T-joints seesaw tested in fluoride mixture NaF–40.0 mole % ZrF_4–6.5 mole % UF_4 for 100 hr at a hot-zone temperature of 816°C

AWS-ASTM classification and braze alloy composition[a]	Weight change[b]		Metallographic notes
	Grams	Percent	
BCu, 100 Cu	–0.0002	–0.026	0.5 mil surface attack along fillet
BNi-3	–0.0008	–0.052	0.5 mil nonuniform surface attack along fillet
BNi-2	–0.0008	–0.063	0.5 mil nonuniform surface attack along fillet
BNi-4	–0.0014	–0.085	0.5 mil uniform surface attack along fillet
70 Ni–13 Ge–11 Cr–6 Si	–0.0011	–0.067	Nonuniform attack of 1.5 mils along surface of braze fillet
	–0.0009	–0.092	1.5 mil uniform surface attack along braze fillet
BNi-1	–0.0005	–0.030	1.5 mil erratic surface attack along braze fillet
BNi-2	–0.0011	–0.092	1.5 mil nonuniform attack along surface of braze fillet
BNi-5	–0.0008	–0.067	3.5 mil attack along surface of braze fillet
65 Ni–25 Ge–10 Cr	–0.0019	–0.056	Stringer-type attack to a maximum depth of 4 mils, few localized areas

[a]Brazing alloys listed in order of decreasing corrosion resistance to the fluoride salt.

[b]Weight-change data for brazing alloy and base material.

Table 8. Results of static tests of brazing alloys on nickel T-Joints in fluoride mixture NaF–40 mole % ZrF_4–6.5 mole % UF_4 at 816°C for 100 hr

AWS-ASTM classification and braze alloy[a] composition	Weight change[b]		Metallographic notes
	Grams	Percent	
BAu-4, 82 Au–18 Ni	–0.0010	–0.036	Braze fillet unattacked
60 Pd–40 Ni	–0.0016	–0.06	No surface attack along braze fillet
60 Pd–37 Ni–3 Si	+0.0008	+0.027	No attack along surface of braze fillet
BNi-7, 10 Cr–10 P–80Ni	0.0	0.0	No attack on braze fillet
50 Ni–25 Mo–25 Ge	0.0	0.0	No attack along surface of braze fillet
BNi-1, 73 Ni–3.5 B–14 Cr–4.5 Fe–4 Si	–0.0004	–0.016	No attack along fillet
BAu-2, 80 Au–20 Cu	–0.0007	–0.026	No attack on braze fillet
75 Ni–25 Ge	–0.0001	–0.01	Max attack of 0.5 mil along surface at fillet
BCu, 100 Cu	–0.0006	–0.019	0.5 mil surface attack along braze fillet
65 Ni–25 Ge–10 Cr	0.0	0.0	Small subsurface voids to a depth of 0.5 mil along braze fillet
BNi-3, 90.5 Ni–3.25 B–1.5 Fe–4.5 Si	–0.0004	–0.05	Nonuniform attack of 6 mils along surface of fillet
BNi-5, 81 Ni–10 Si–13 Cr	–0.0003	–0.012	Nonuniform attack of 12 mils along fillet
35 Ni–55 Mn–10 Cr	–0.0111	–0.48	Complete attack of braze fillet
40 Ni–60 Mn	–0.0159	–0.59	Complete attack of braze fillet
68 Ni–32 Sn	–0.0998	–3.49	Joint partially dissolved at fillet surface

[a]Brazing alloys listed in order of decreasing corrosion resistance to fluoride mixture.

[b]Weight-change data for brazing alloys and base material of joint.

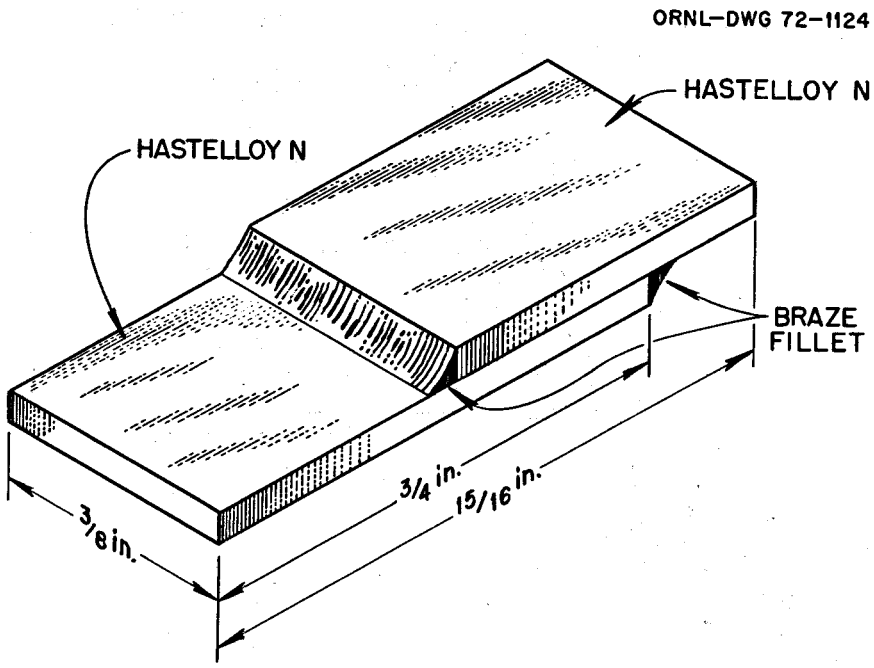

Fig. 1. Lap joint configuration of braze alloy specimens.

4. RESULTS

The weight changes of the specimens as a function of time are given in Fig. 2 and Table 9. Over the entire test, all specimens gained weight: a maximum of 0.024 g and a minimum of 0.014 g or 0.5 to 1.0%. Weight losses for some specimens were seen in the time period between 1141 and 1471 hr and between 2978 hr and the end of the test. A defective pressure gage between a helium cylinder and the test vessel was found at 1471 hr and replaced. This failure probably allowed moisture into the system, which would have caused increased attack (weight loss). No cause for increased oxidation was found for the latter time period.

The salt analysis as a function of time is given in Table 10. Very small changes in impurity content are noted. Little if any significant changes were noted during the periods of increased weight loss.

Figure 3*a* shows a macrograph of the specimens after test (on bottom) as compared with identical specimens untested (on top). Figure 3*b* shows a close-up of a tested (right) and untested (left) specimen. The deposits leading to the overall weight gains can be seen at this magnification ($4\frac{1}{2}$X).

As mentioned earlier, two brazed specimens (lap joint between two Hastelloy N pieces) were made for each braze alloy. Thus we were able to compare the braze microstructure after test with that of the specimen prepared at the same time but not tested. Since the fillet size for each specimen before test may not have been identical, we must necessarily restrict our observations to gross changes. In making judgments on the appearance of the microstructure, two effects must be considered: (1) the corrosive action of the salt and (2) the aging of the braze due to its prolonged exposure at temperature. Percentages of elements in phases were determined by electron probe microanalyzer. No element below the atomic number of sodium could be determined.

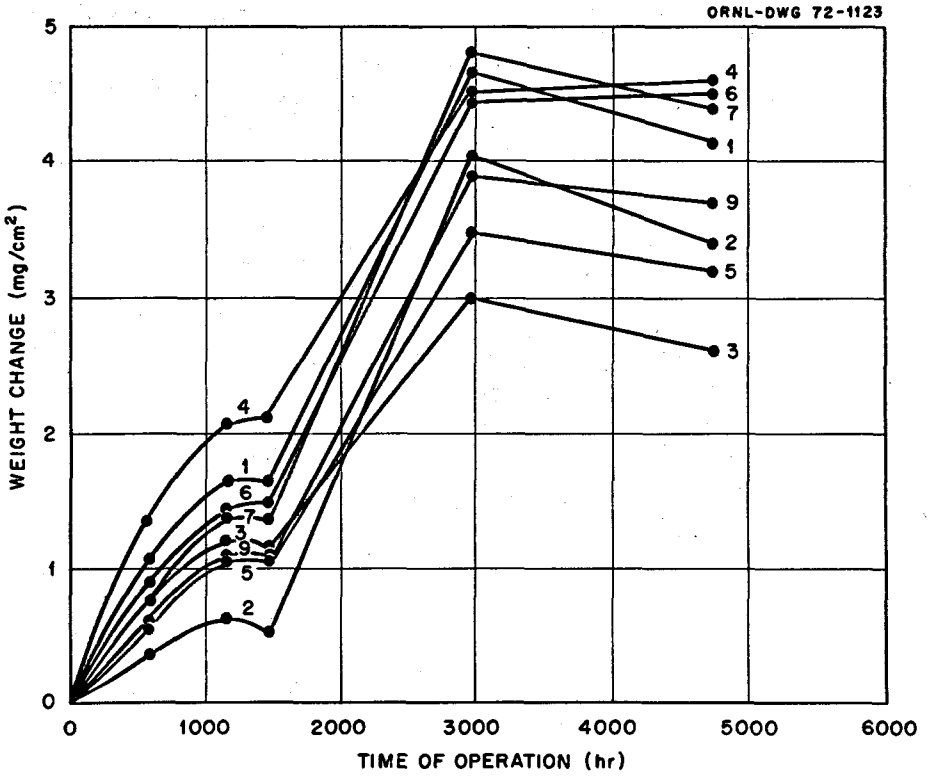

Fig. 2. Weight change of braze alloy specimens as a function of time.

Table 9. Specimen weight changes as a function of time

Specimen No.	Weight changes (g)					
	First 594 hr	Next 547 hr	Next 330 hr	Next 1507 hr	Next 1798 hr	Total 4776 hr
1	+0.0056	+0.0031	−0.0001	+0.0160	−0.0025	+0.0221
2	+0.0019	+0.0014	−0.0006	+0.0188	−0.0036	+0.0179
3	+0.0041	+0.0023	−0.0003	+0.0098	−0.0023	+0.0136
4	+0.0072	+0.0038	+0.0002	+0.0127	+0.0005	+0.0244
5	+0.0028	+0.0027	+0.0001	+0.0128	−0.0013	+0.0171
6	+0.0047	+0.0029	+0.0003	+0.0157	+0.0005	+0.0241
7	+0.0041	+0.0033	−0.0001	+0.0181	−0.0018	+0.0236
9	+0.0032	+0.0026	−0.0001	+0.0150	−0.0013	+0.0194

Table 10. Analysis of salt

Time (hr)	Percent			Parts per million					
	Na	B	F	Cr	Fe	Ni	Mo	O_2	H+
As received	21.6	9.78	68.9	12	294	32	<2	480	22
570	22.1	9.73	69.1	7	192	33	<2	490	19
1199	22.9	9.54	69.3	15	193	41	<2	640	29
1632	21.1	9.93	68.7	14	193	26	2	532	19
2978	20.9	9.24	89.0	16	252	48	65	609	24
4991	22.5	9.46	68.76	15	264	82	5	699	16

All other elements <2 ppm.

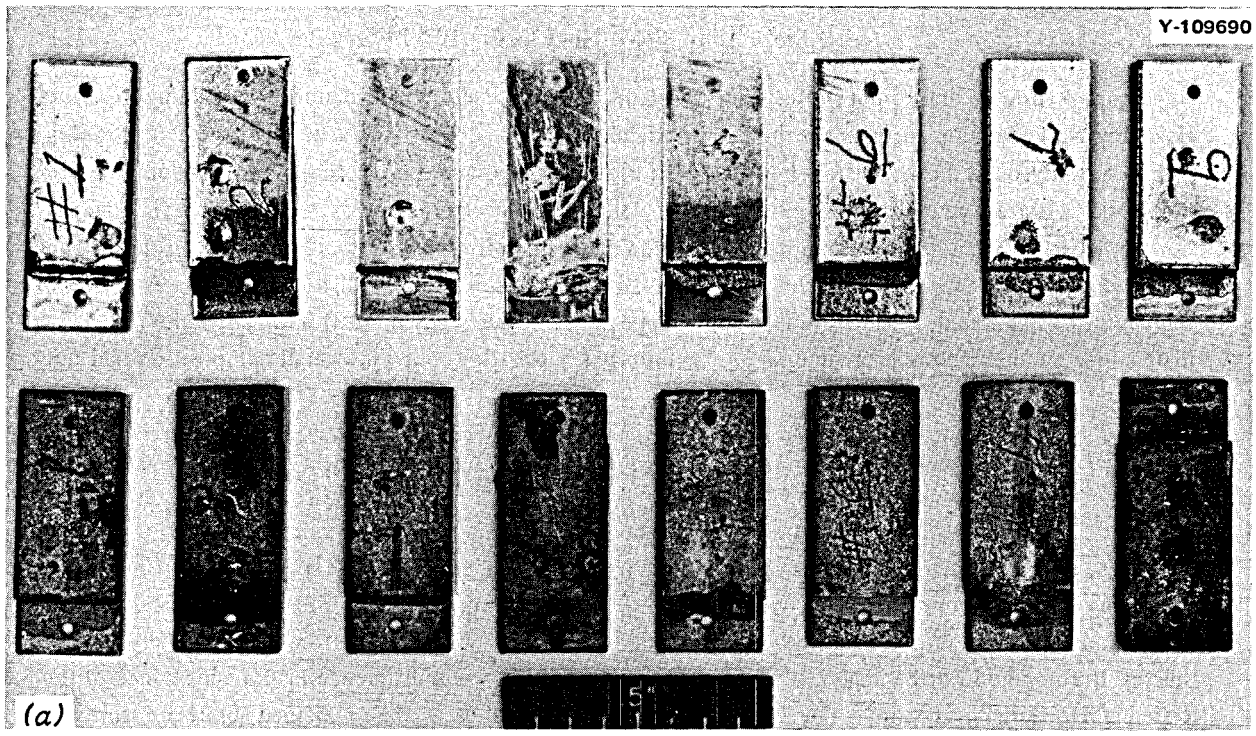

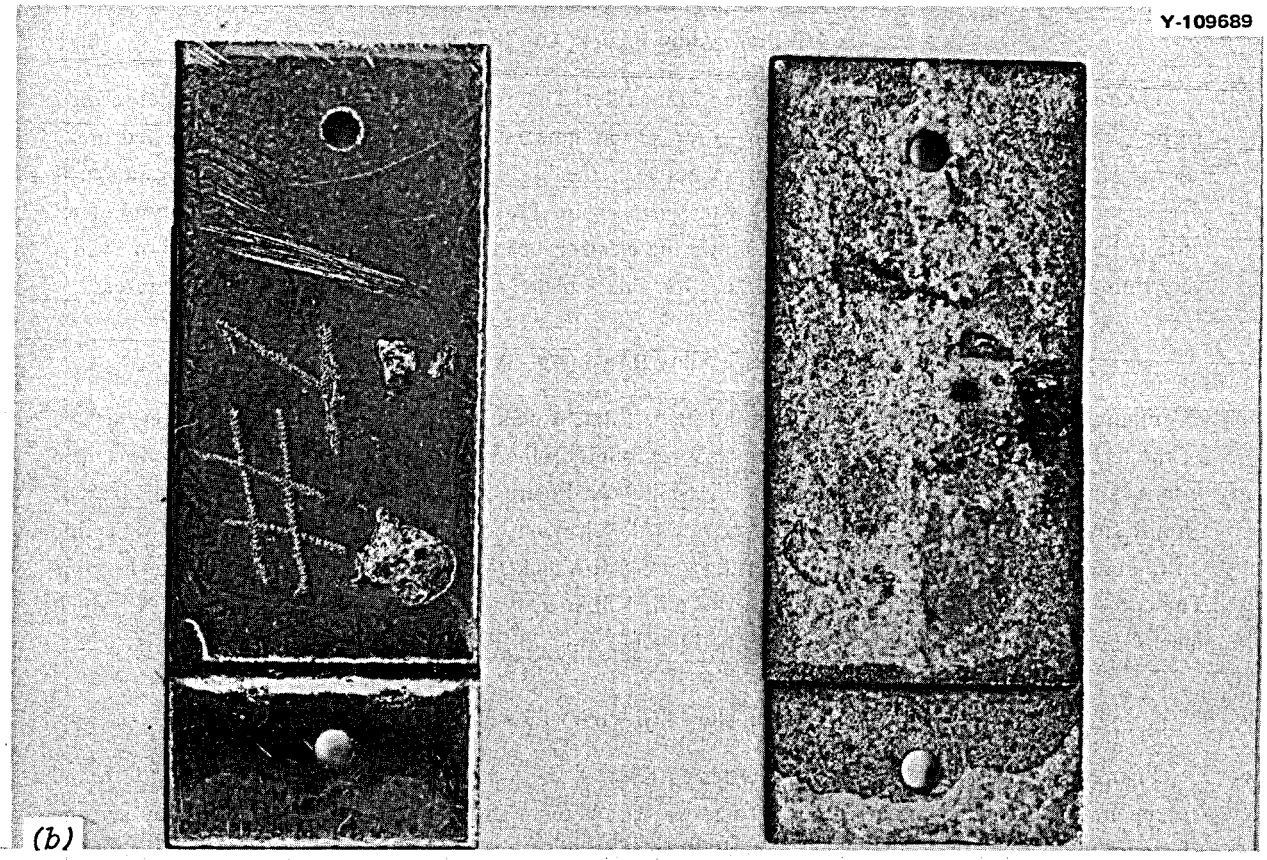

Fig. 3. Braze alloy specimen. (*a*) As-brazed – top, exposed to $NaBF_4$–8 mole % NaF at 610°C for 4987 hr – bottom, 1½×; (*b*) as-brazed – left, tested – right, 4½×.

4.1 Braze Alloy BNi-7 (Ni–13% Cr–10% P)

Figure 4 shows a braze fillet (untested and tested). Both braze alloys have dendrites extending from the Hastelloy N. The major difference is the color of dendrites, which could be an artifact. Large deposits, seen in Fig. 5, were found on the Hastelloy N after test. Figure 5 shows a microstructural analysis of an untested braze and a braze exposed to the salt, and Fig. 6 shows the electron beam scanning images. The largest deviation from the basic alloy composition occurred in dark dendrites, which were poor in phosphorus and rich in chromium, extending from the Hastelloy N. They were similar to the light-colored phases found in the center of the tested braze alloy. The overall appearance of the braze microstructure after the test was a little different than the microstructure of the untested braze alloy, but the overall composition had not changed.

4.2 Braze Alloy BNi-3 (Ni–3.5% Fe–4.5% Si–2.9% B)

Figure 7 shows an untested and a tested braze fillet. Certain phases are more defined in the tested specimen. Small deposits were found on the Hastelloy N after test, and there was some interdiffusion at the Hastelloy N–braze-alloy interface. Figure 8 shows the microstructural analysis of an untested and a tested braze, and Fig. 9 shows the electron beam scanning images. The phases rich in iron were generally poor in silicon. Boron could not be analyzed. Again, even though there was a difference in the appearance of the tested and untested braze alloys, the compositions and amounts of each phase remained about the same.

4.3 Braze Alloy BAu-4 (Au–18% Ni)

Figure 10 shows an untested and a tested braze fillet. The exposure surface of the tested fillet seemed to be somewhat roughened, with a slight difference in appearance of the as-brazed and the tested braze alloys. There appears to be little interaction between the braze alloy and the Hastelloy N. Again, small deposits were found on the Hastelloy N after test. Figure 11 shows the microstructural analysis of an untested and a tested braze, and Fig. 12 shows the electron beam scanning image. The tested braze had a very thin nickel deposit on its exposed surface. Some dark nickel-rich phases were found in both brazes.

4.4 Braze Alloy BAg-8 (Ag–28% Cu)

Figure 13 shows an untested and a tested braze fillet. A deposit was evident along the exposed surface of the tested braze alloy. Again, small deposits were found on the Hastelloy N after test, and there was little interaction between the braze alloy and the Hastelloy N. Figure 14, shows the microstructural analysis of an untested and a tested braze, and Fig. 15 shows the electron beam scanning image. Both phases making up the eutectic braze alloy are easily identified along with nickel-containing phases formed during brazing. The composition of the surface deposit of the tested fillet analyzed as 9% Ag, 41% Cu, and 50% Ni, which means that the deposited material was essentially nickel which diffused into the braze alloy.

4.5 Braze Alloy BNi-4 (Ni–4.5% Si–3% B)

Figure 16 shows the as-brazed and the tested fillet. A large amount of fillet was missing in the tested specimen, but the actual fillet size before test was not known. Diffusion between the braze alloy and the Hastelloy N is evident. Rather large deposits were found on the Hastelloy N; Fig. 16*c* shows a typical deposit. The microstructural analysis is seen in Fig. 17, and one phase with 11% Si is noted. Boron could not be analyzed. The areas of large concentrations of silicon are seen in Fig. 18.

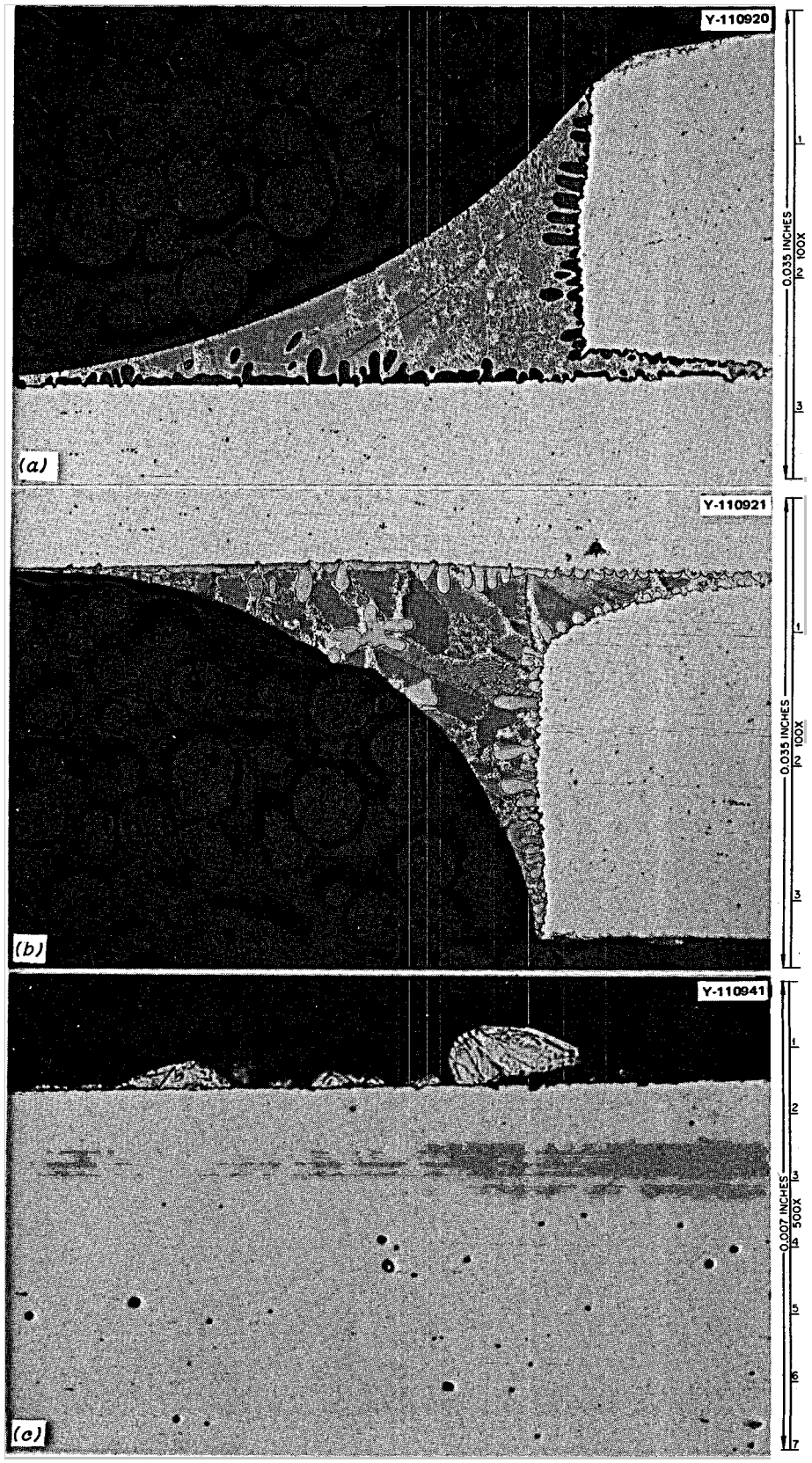

Fig. 4. Braze alloy BNi-7 (Ni–13% Cr–10% P)-Hastelloy N. As-polished. 100X. (*a*) As-brazed; (*b*) exposed to $NaBF_4$–8 mole % NaF for 4987 hr at 610°C; (*c*) deposit on Hastelloy N after test.

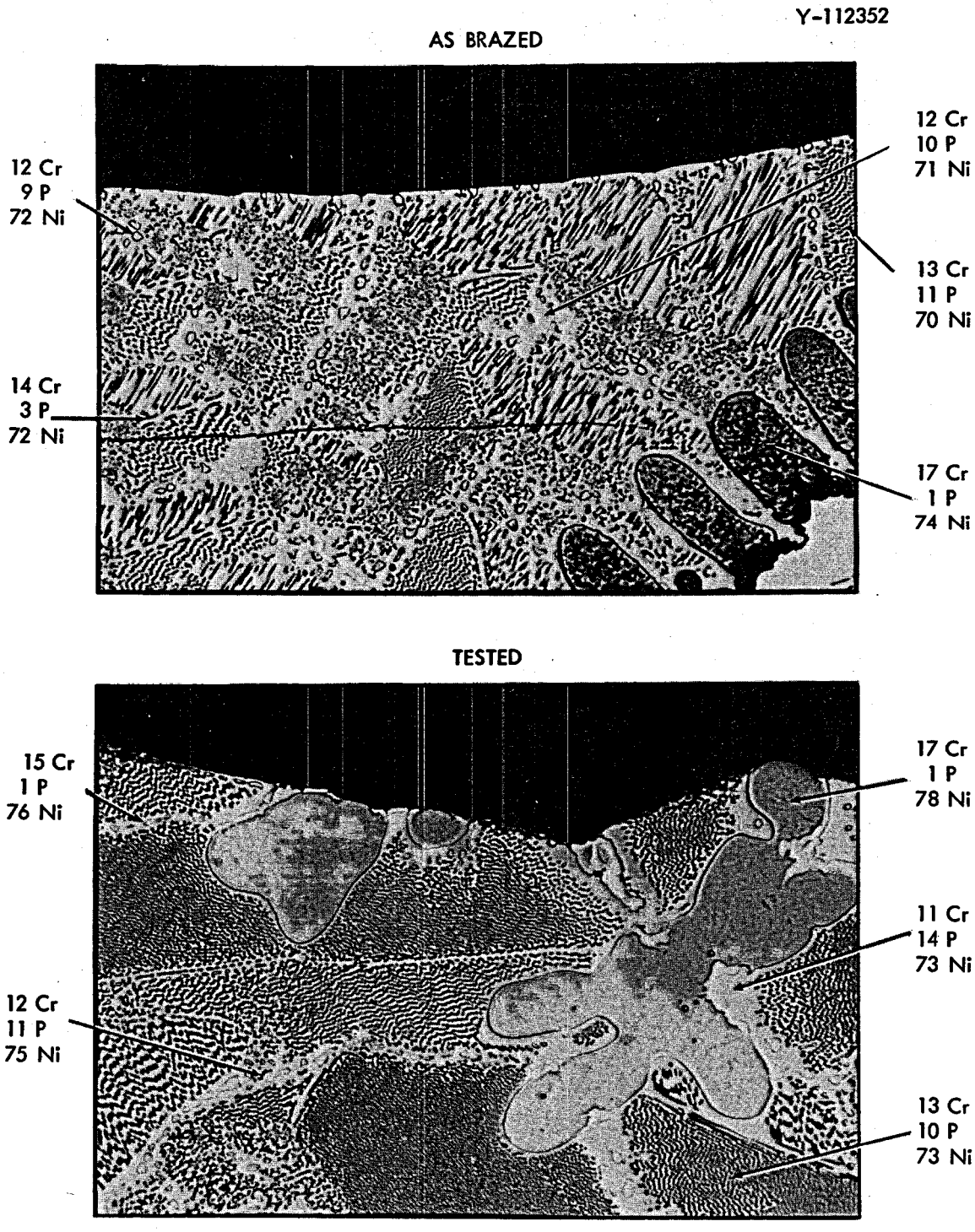

Fig. 5. Microstructural analysis of BNi-7 (Ni–13% Cr–10% P) braze fillet. As-polished. 500X. Top – as-brazed; bottom – exposed to $NaBF_4$–8 mole % NaF for 4987 hr at 610°C. Reduced 19%.

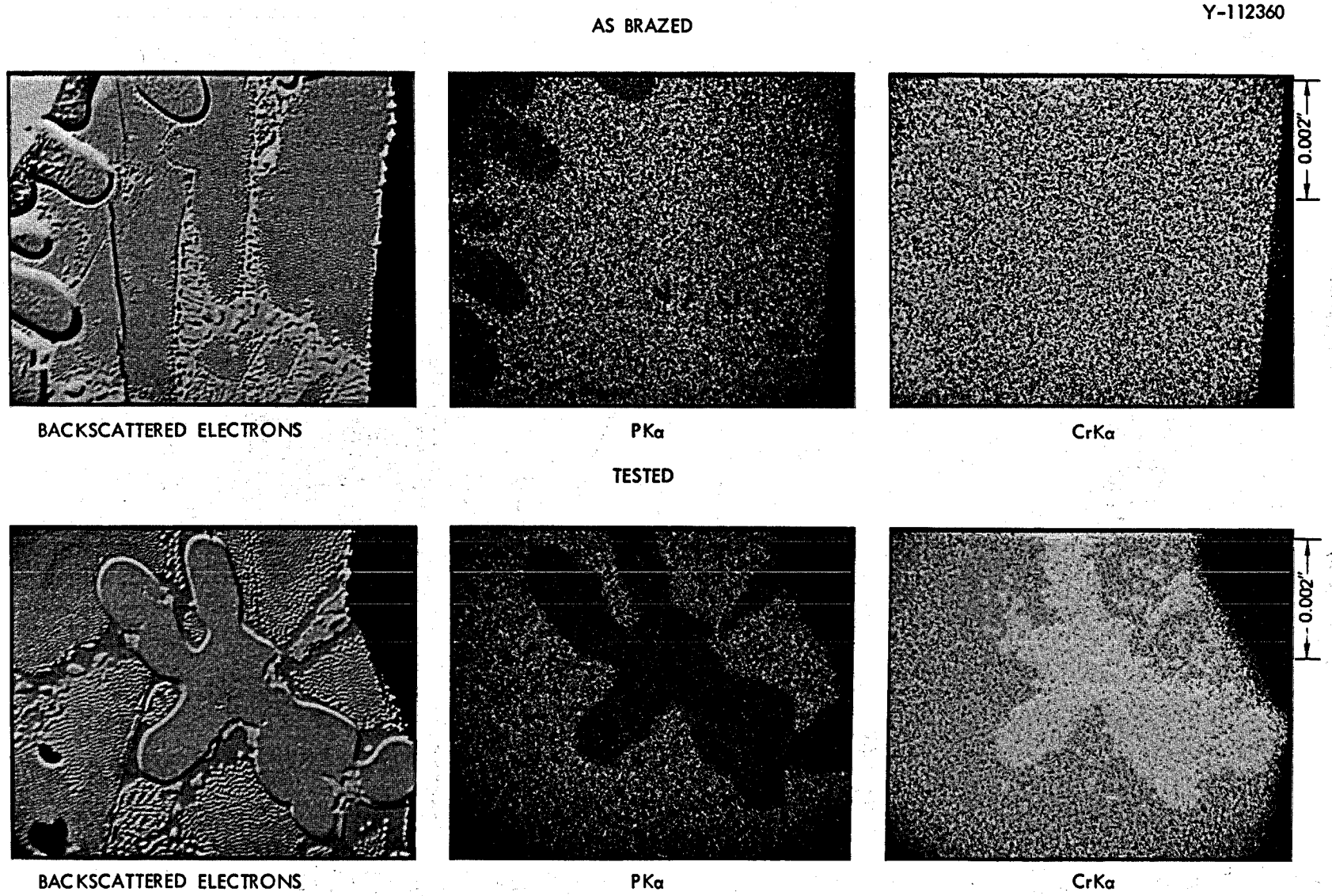

Fig. 6. Electron-beam scanning images of BNi-7 (Ni–13% Cr–10% P) braze fillet. Top – as-brazed; bottom – exposed to $NaBF_4$–8 mole % NaF for 4987 hr at 610°C.

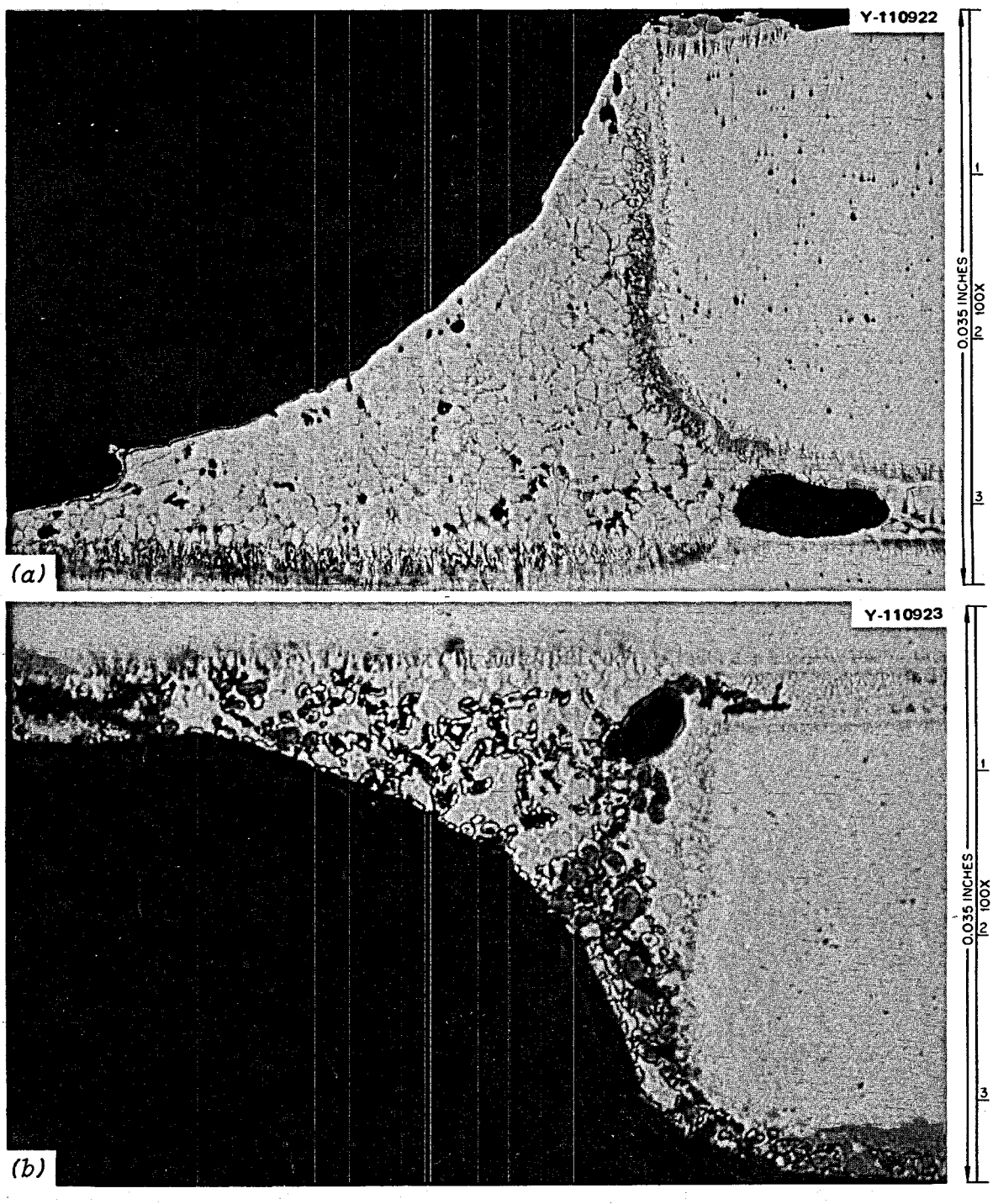

Fig. 7. Braze alloy BNi-3 (Ni–4.5% Si–3.5% Fe–2.9% B) Hastelloy N. As-polished. 100X. (*a*) As-brazed; (*b*) exposed to $NaBF_4$–8 mole % NaF for 4987 hr at 610°C.

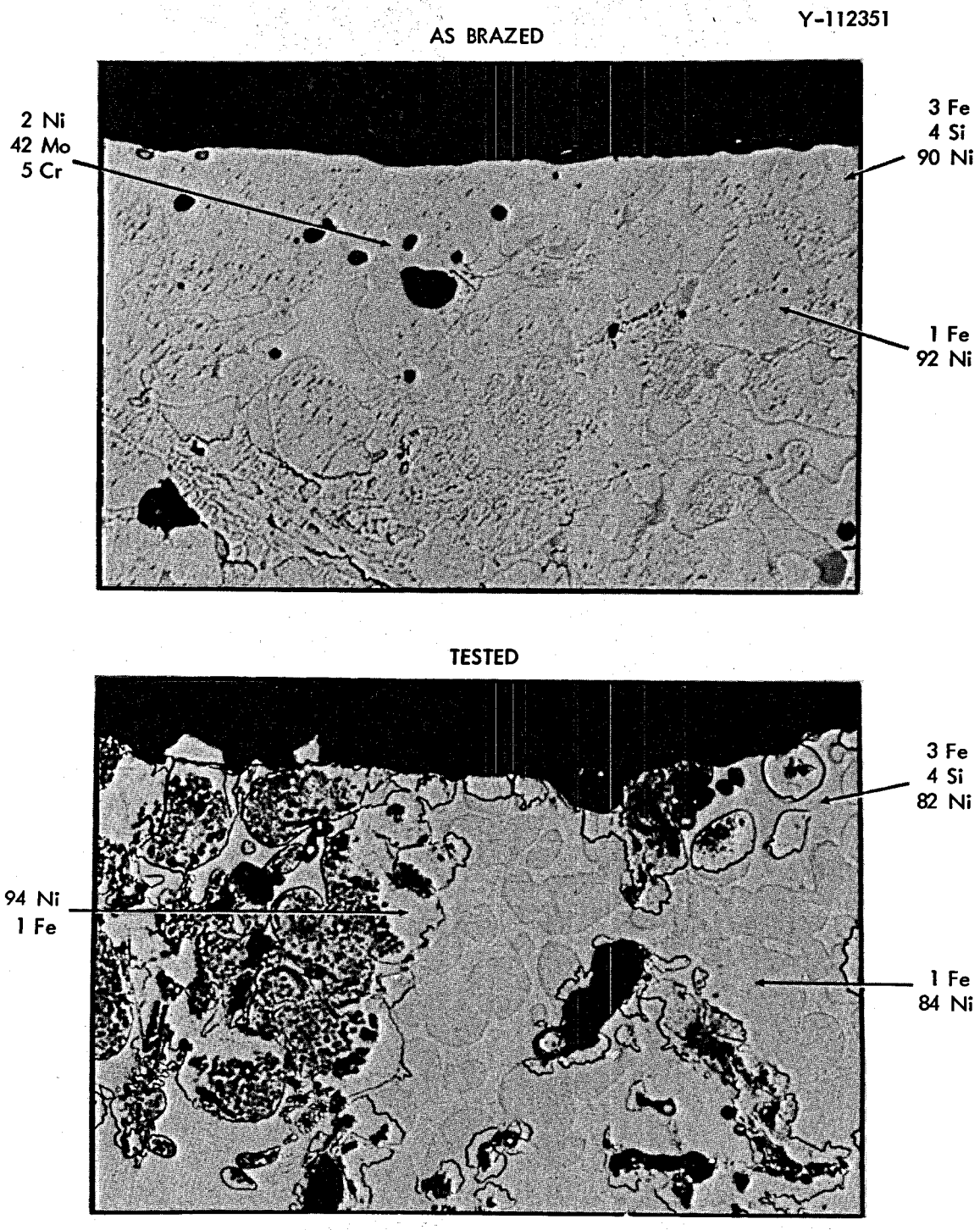

Fig. 8. Microstructural analysis of BNi-3 (Ni–4.5% Si–3.5% Fe–2.9% B) braze fillet. Top – as-brazed; bottom – exposed to $NaBF_4$–8 mole % NaF for 4987 hr at 610°C.

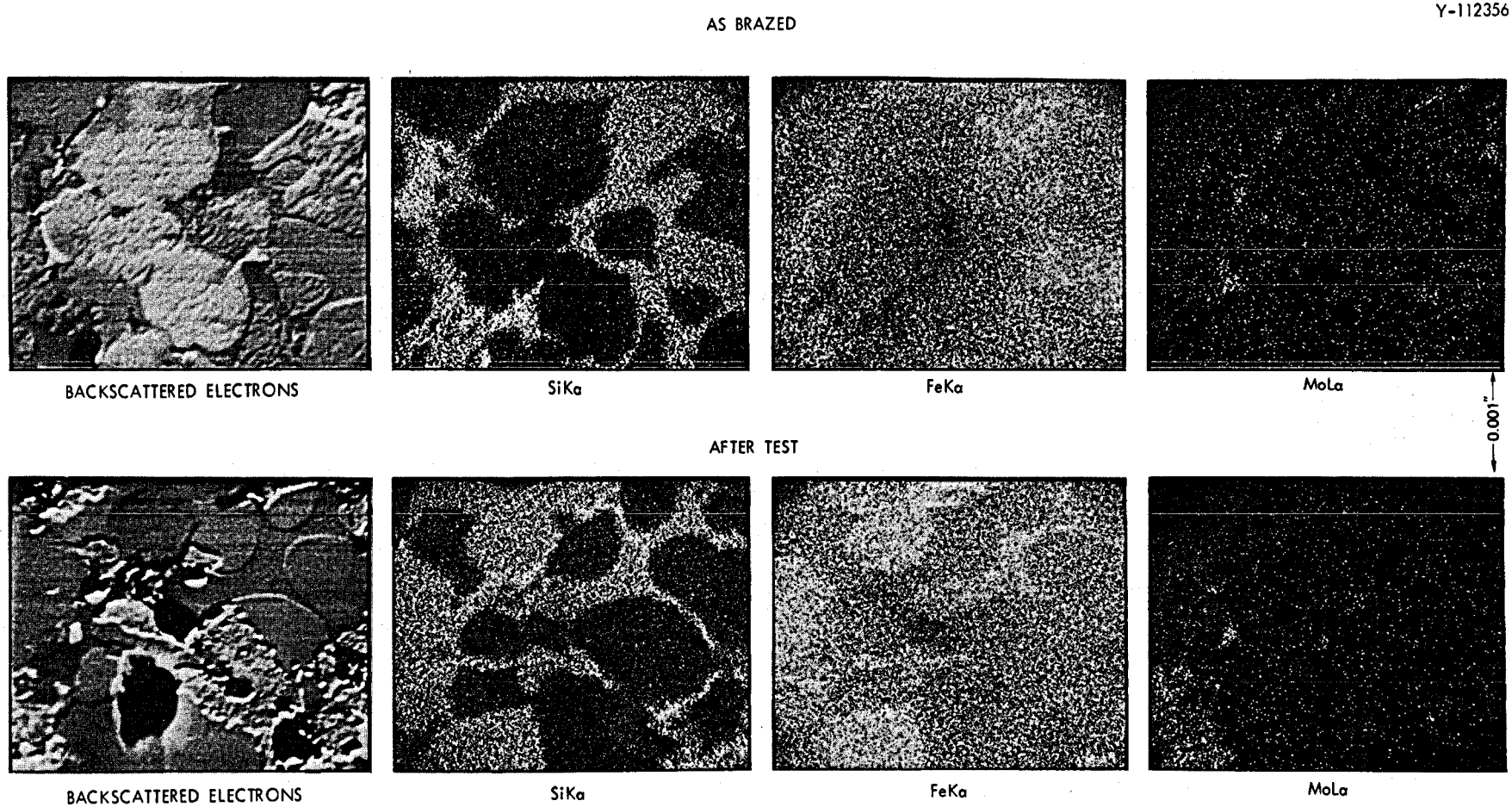

Fig. 9. Electron-beam scanning images of BNi-3 (Ni–4.5% Si–3.5% Fe–2.9% B) braze fillet. Top – as-brazed; bottom – exposed to $NaBF_4$–8 mole % NaF for 4987 hr at 610°C.

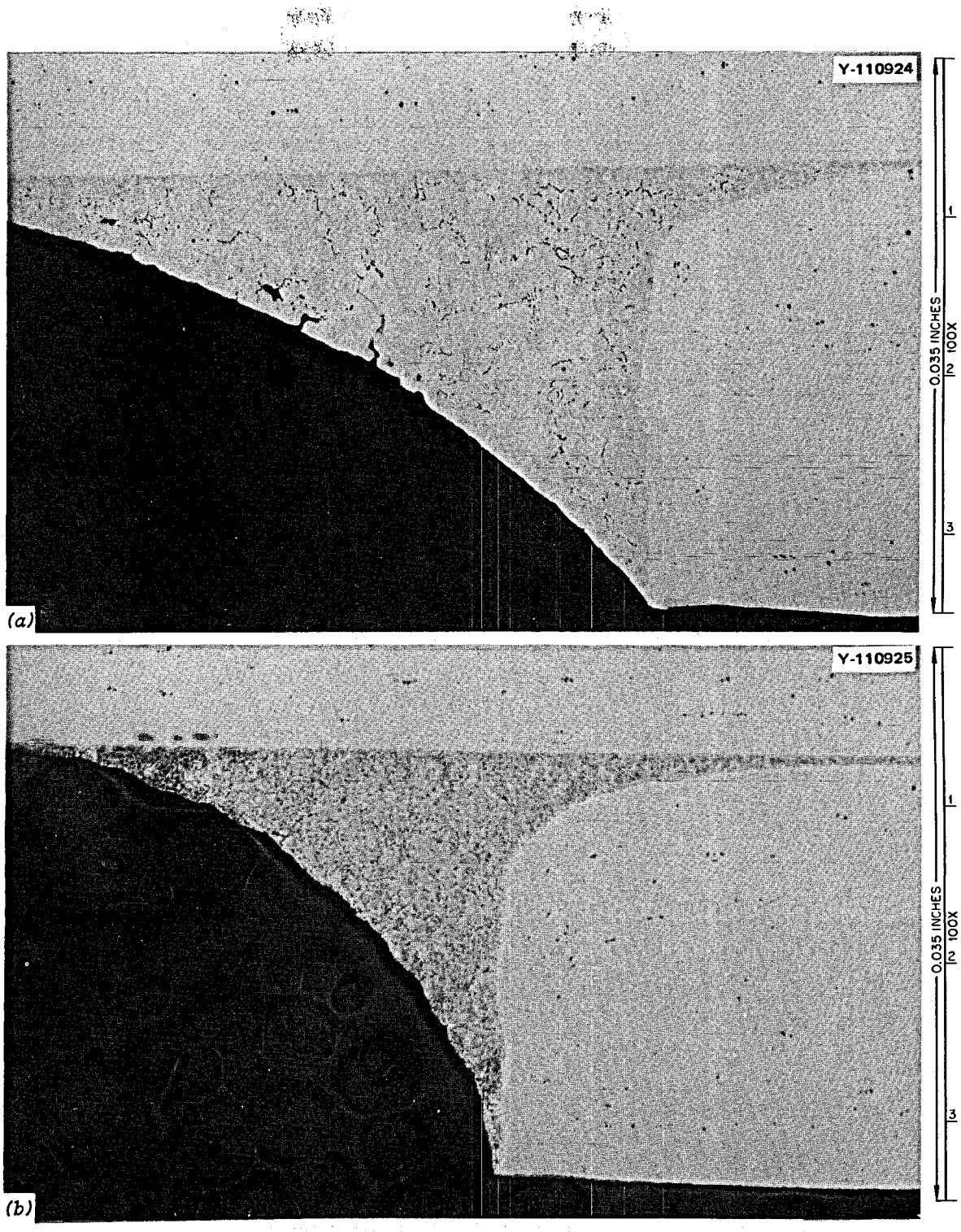

Fig. 10. Braze alloy BAu-4 (Au–18% Ni) Hastelloy N. As-polished. 100X. (*a*) As-brazed; (*b*) exposed to $NaBF_4$–8 mole % NaF for 4987 hr at 610°C.

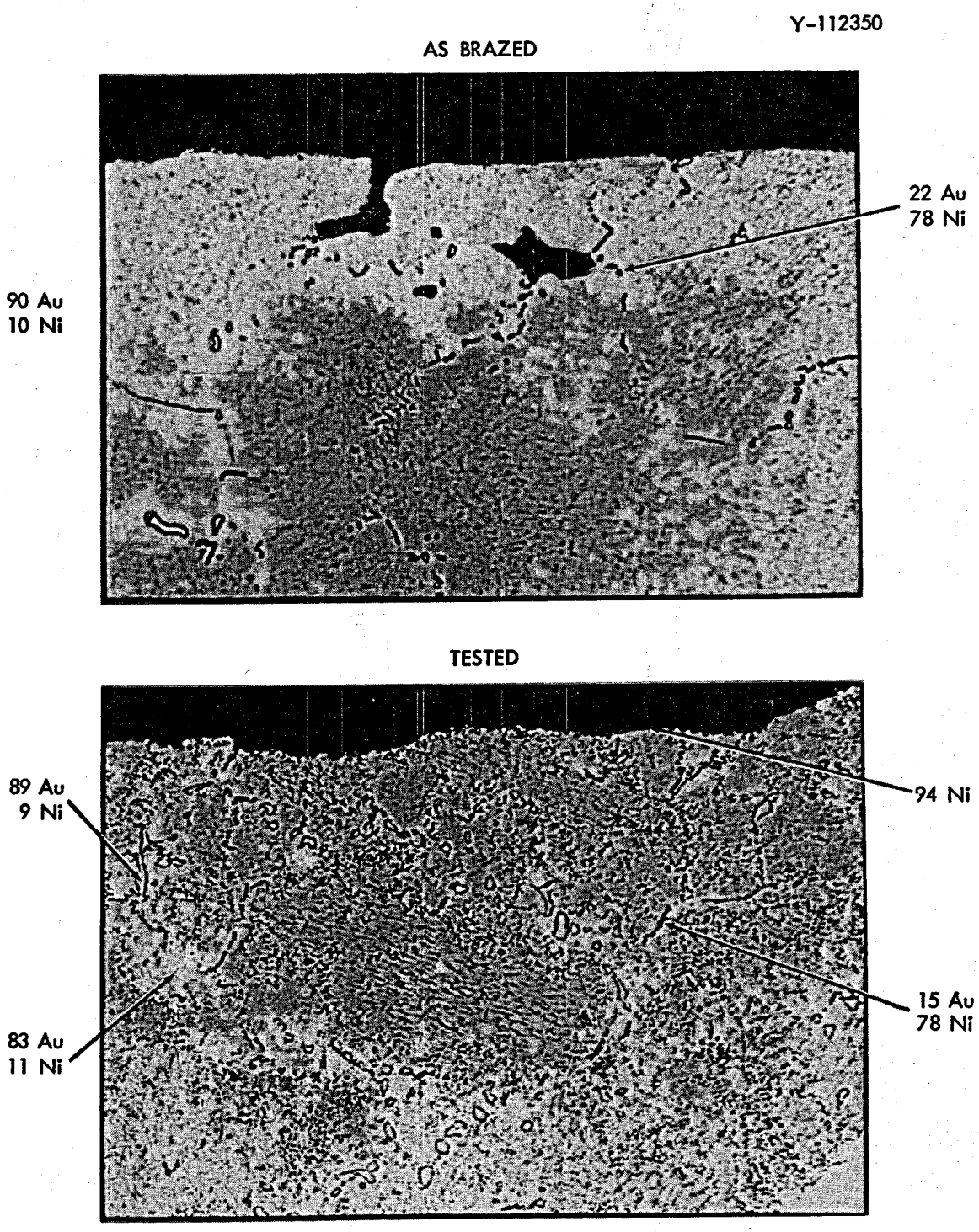

Fig. 11. Microstructural analysis of BAu-4 (Au–18% Ni) braze fillet. Top – as-brazed; bottom – exposed to $NaBF_4$–8 mole % NaF for 4987 hr at 610°C.

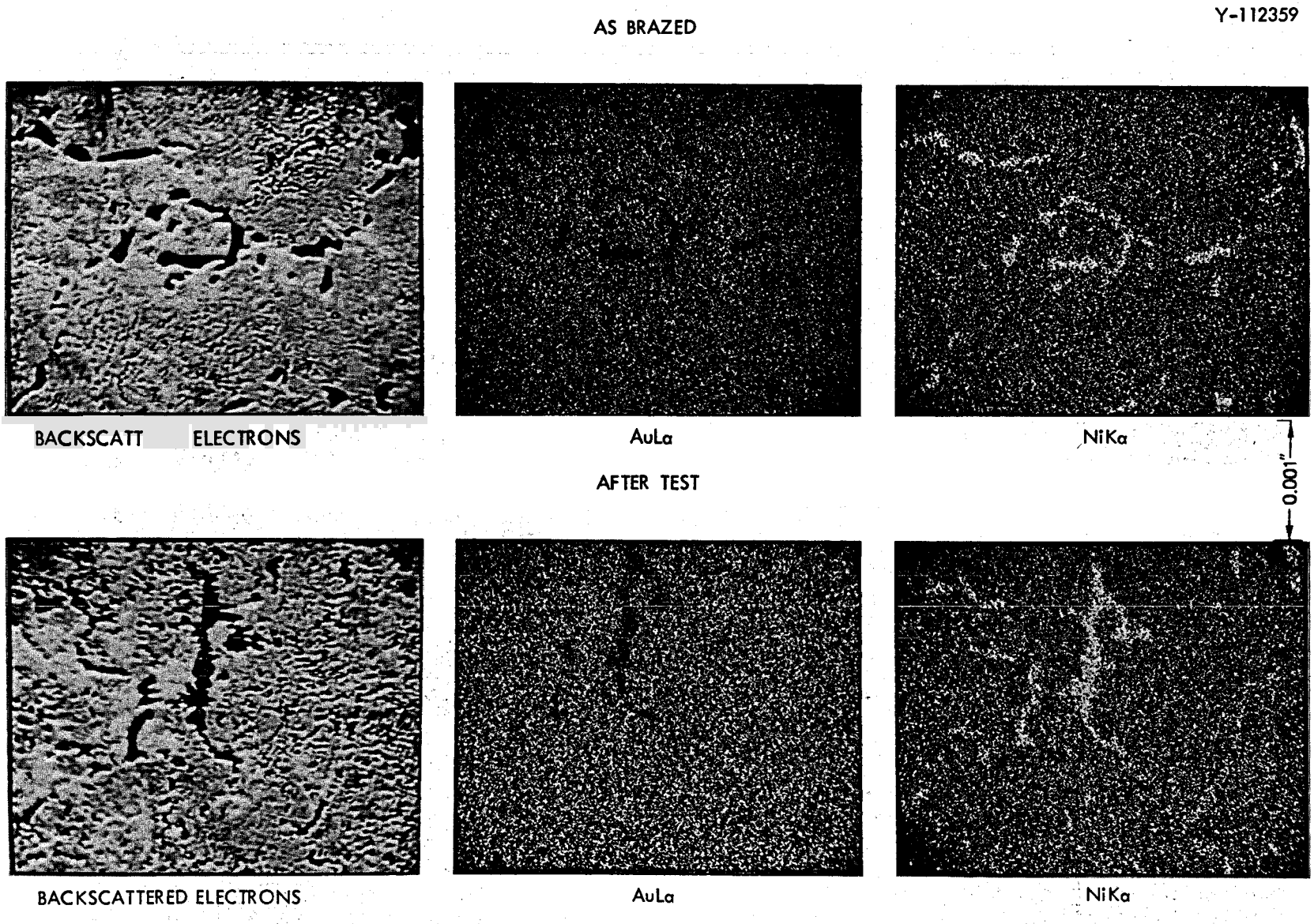

Fig. 12. Electron-beam scanning images of BAu-4 (Au–18% Ni) braze fillet. Top – as-brazed; bottom – exposed to $NaBF_4$–8 mole % NaF for 4987 hr at 610°C.

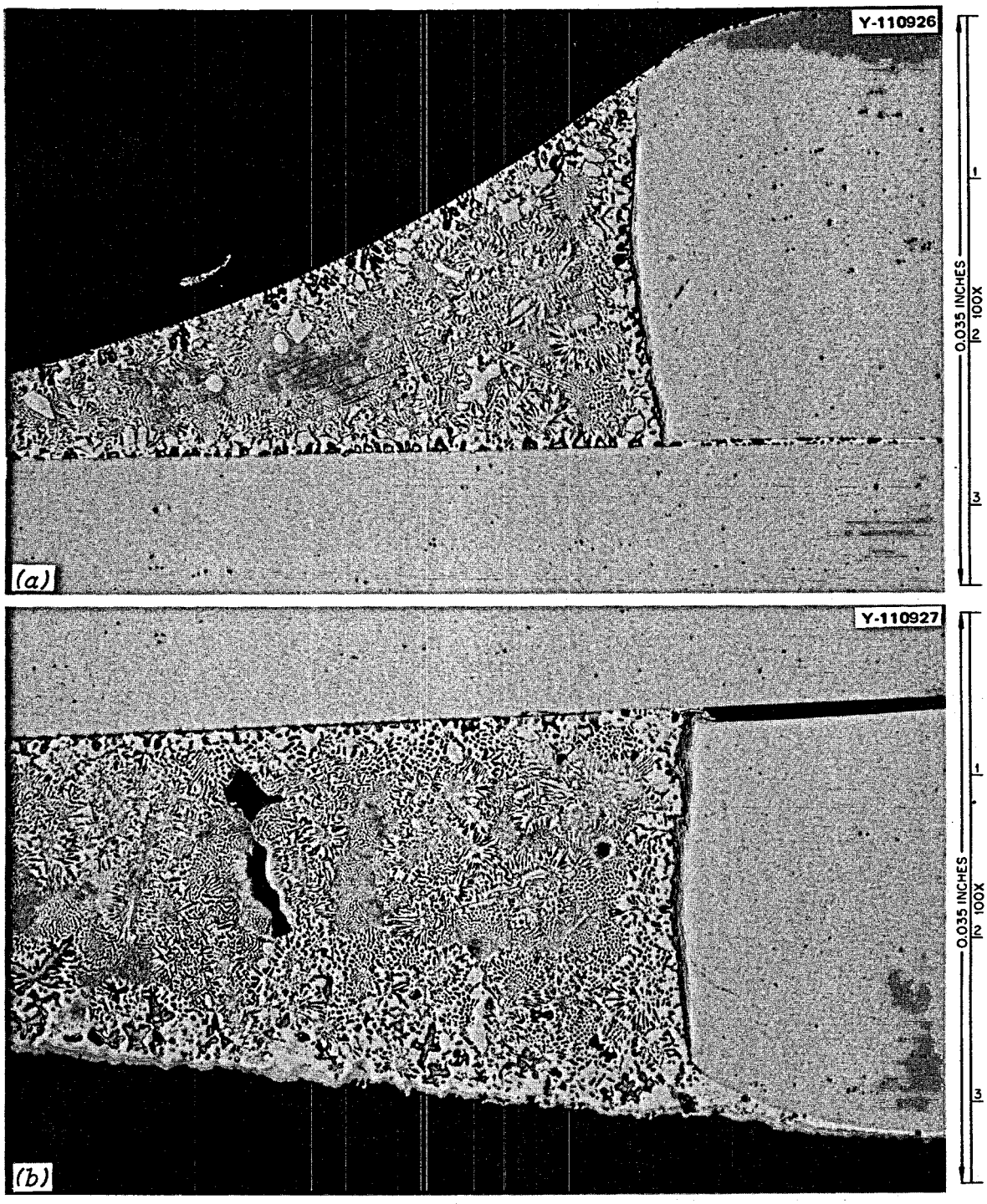

Fig. 13. Braze alloy BAg-8 (Ag–28% Cu) Hastelloy N. As-polished. 100×. (*a*) As-brazed; (*b*) exposed to $NaBF_4$–8 mole % NaF for 4987 hr at 610°C.

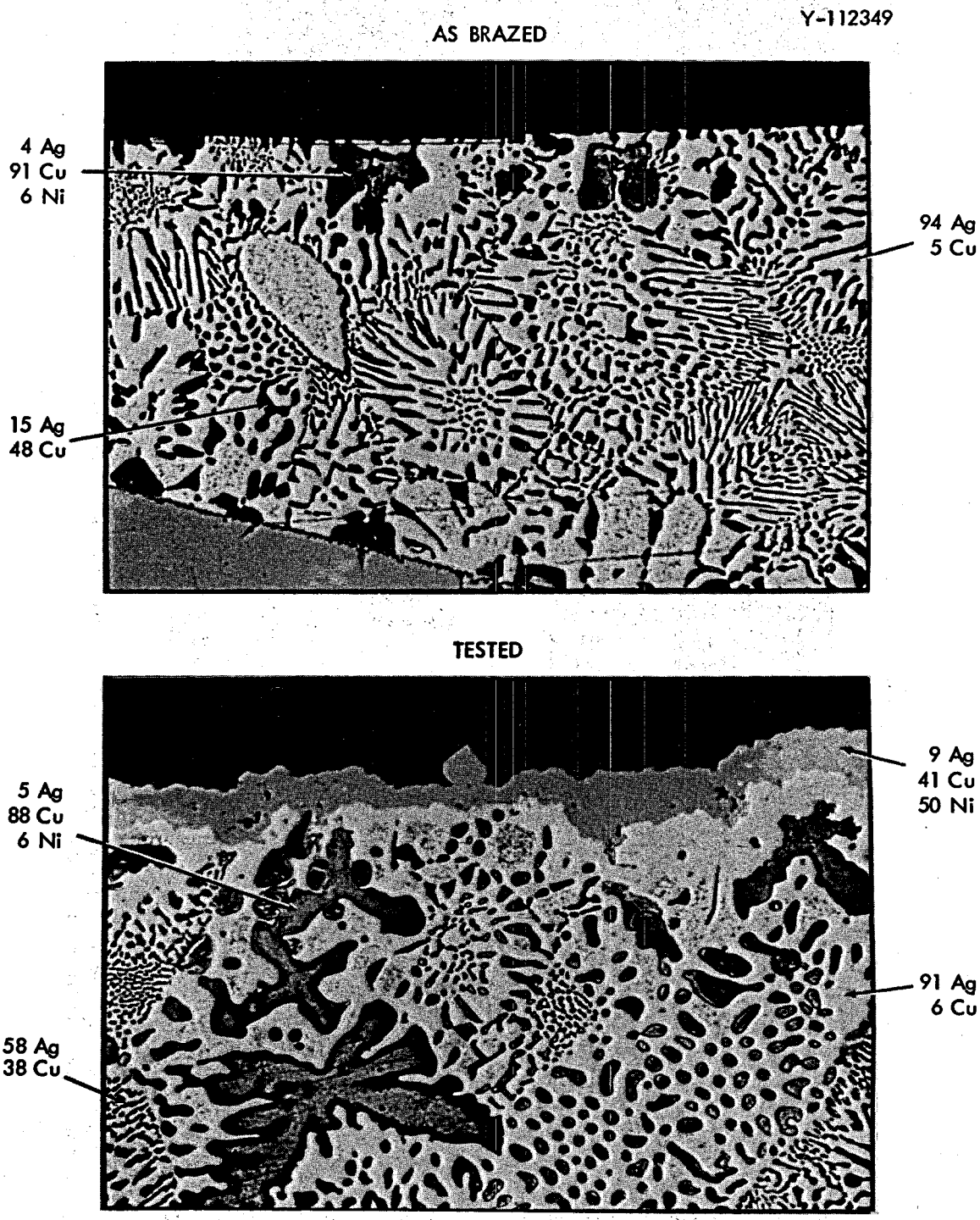

Fig. 14. Microstructural analysis of BAg-8 (Ag–28% Cu) braze fillet. Top – as brazed; bottom – exposed to $NaBF_4$–8 mole % NaF for 4987 hr at 610°C.

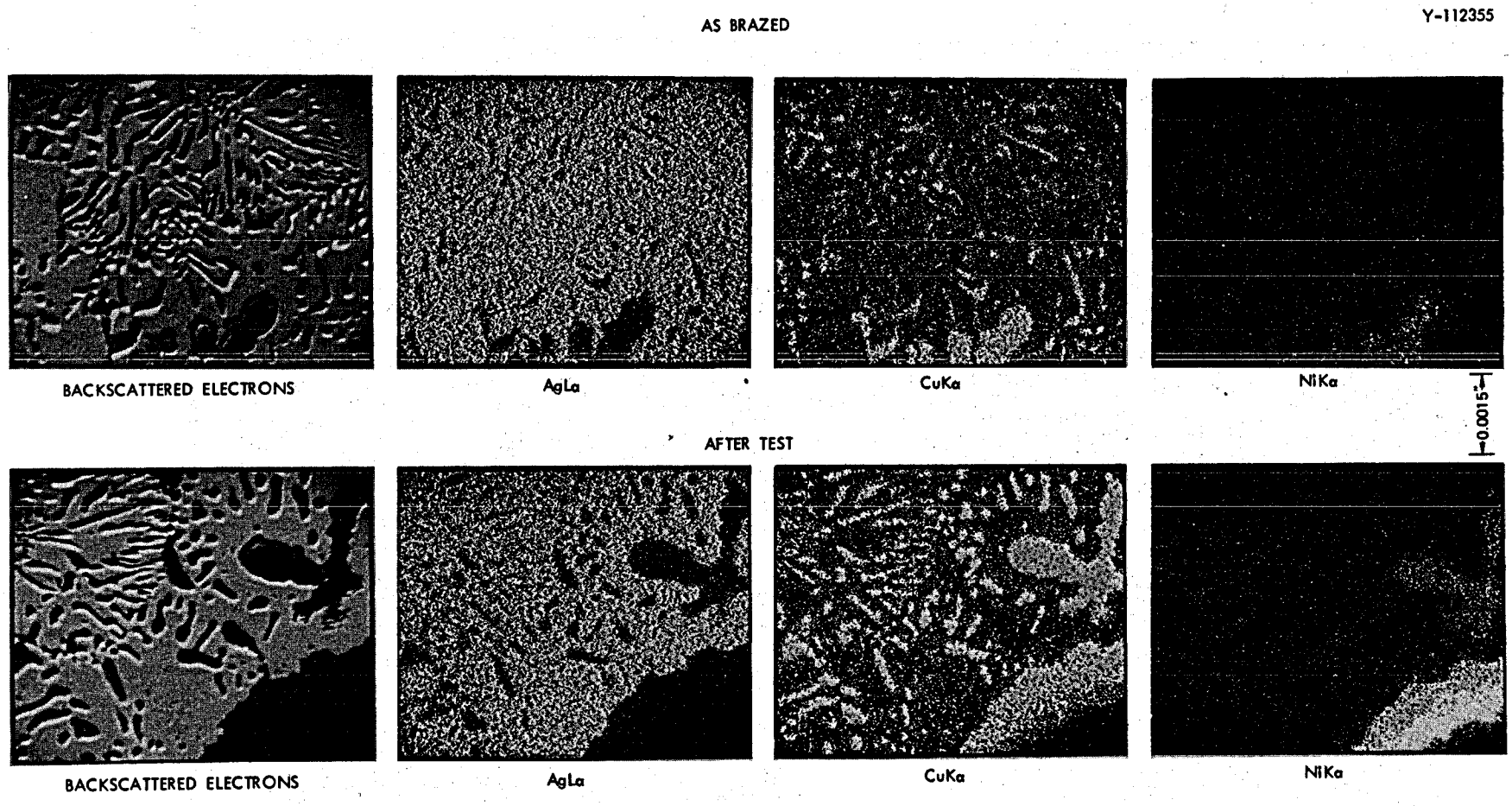

Fig. 15. Electron-beam scanning images of BAg-8 (Ag–28% Cu) braze fillet. Top – as-brazed; bottom – exposed to $NaBF_4$–8 mole % NaF for 4987 hr at 610°C.

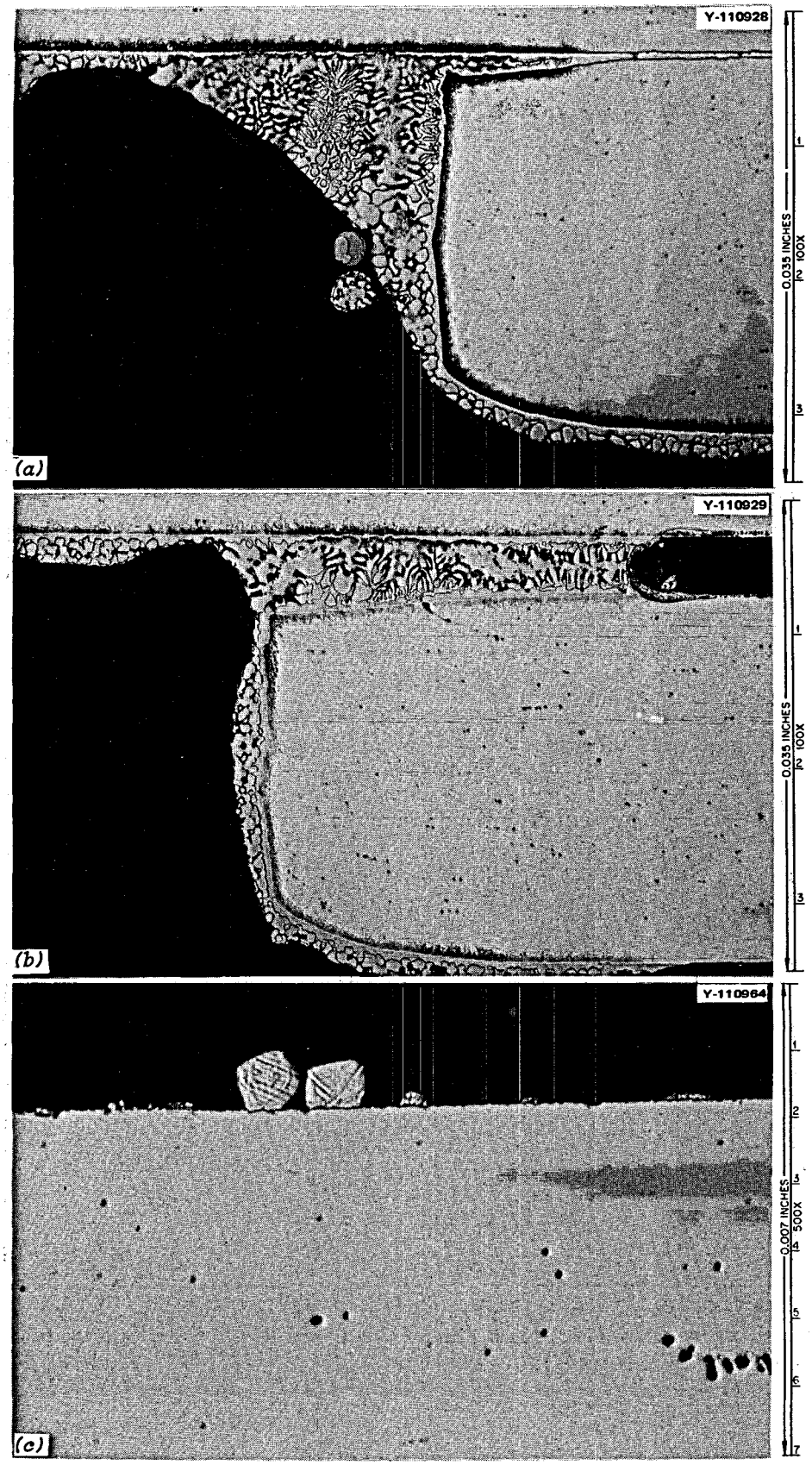

Fig. 16. Braze alloy BNi-4 (Ni–4.5% Si–3.0% B) Hastelloy N. As-polished. 100×. (*a*) As-brazed; (*b*) exposed to $NaBF_4$–8 mole % NaF for 4987 hr at 610°C; (*c*) deposit on Hastelloy N after test.

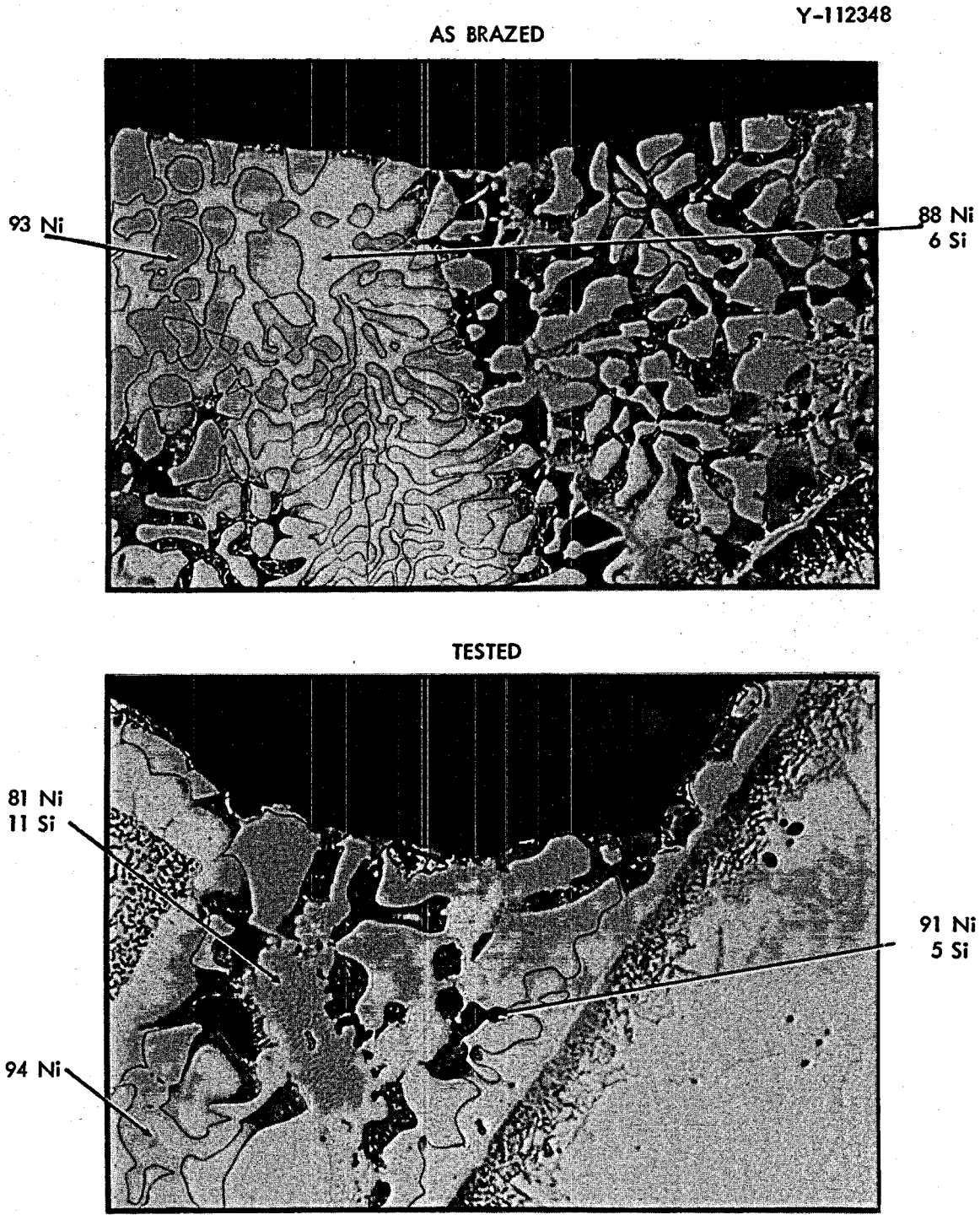

Fig. 17. Microstructural analysis of BNi-4 (Ni–4.5% Si–3.0% B) braze fillet. Top – as-brazed; bottom – exposed to $NaBF_4$–8 mole % NaF for 4987 hr at 610°C.

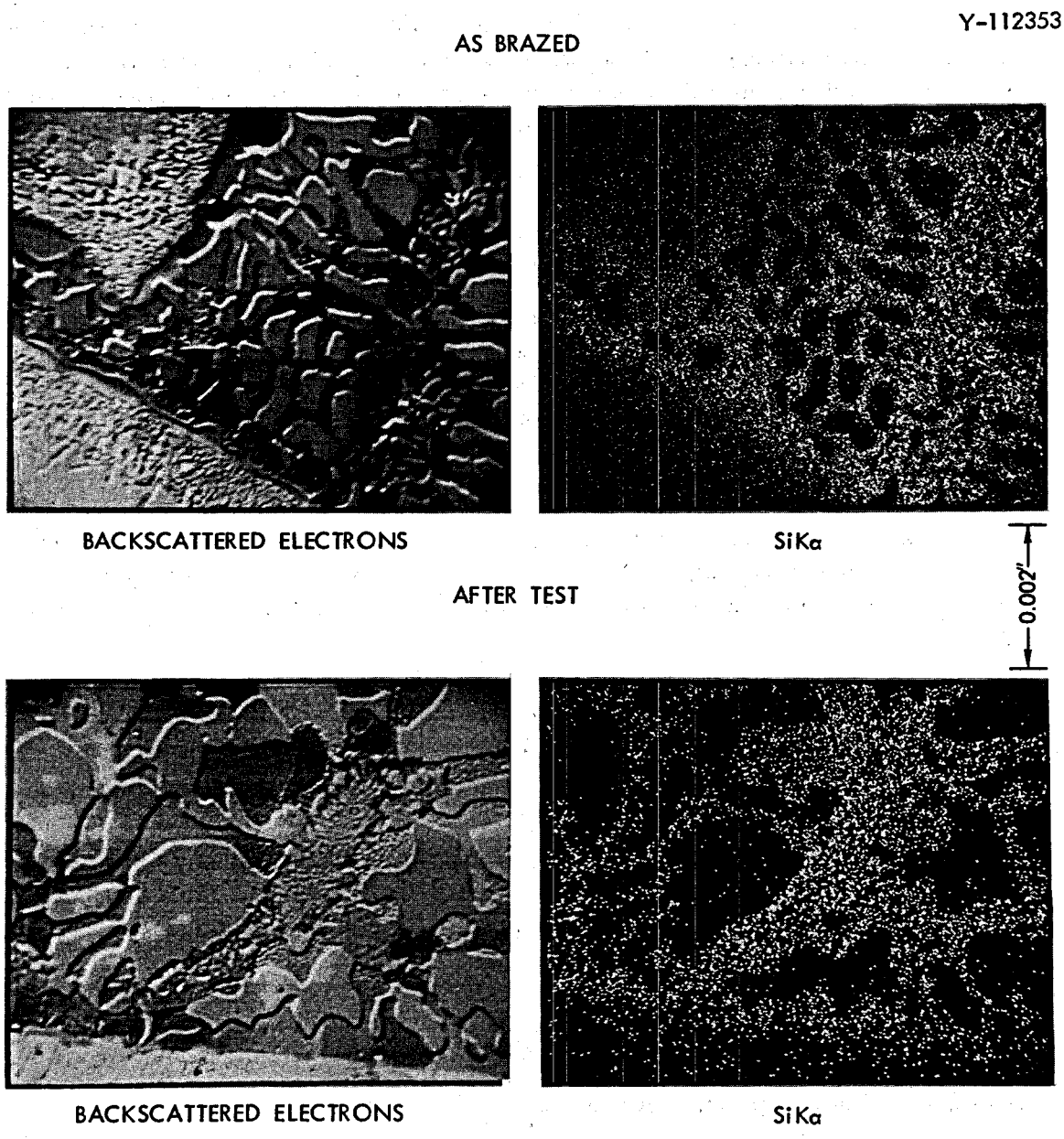

Fig. 18. Electron-beam scanning images of BNi-4 (Ni–4.5% Si–3.0% B) braze fillet. Top – as-brazed; bottom – exposed to $NaBF_4$–8 mole % NaF for 4987 hr at 610°C.

4.6 Braze Alloy BCu (100% Cu)

Figure 19 shows the as-brazed and the tested fillet. A deposit was noted along the exposed surface of the tested braze alloy. Little interaction between braze and base metal is noted. Larger deposits were found on the Hastelloy N after test; Fig. 19*c* shows a typical deposit. The microstructural analysis shown in Fig. 20 shows constituents of the Hastelloy N base material mixed with the copper for both the tested and the as-brazed material. The composition of the surface deposit of the tested fillet consists of equal amounts of copper and nickel, with a smaller amount of nickel as you go from the surface. This probably means that nickel is deposited on the surface during exposure and diffused in. The extent of the mixing of the nickel and molybdenum in the matrix of the fillet before exposure is seen in the electron beam scanning images of Fig. 21.

4.7 Braze Alloy BNi-2 (Ni–7.0% Cr–3.5% Fe–4.5% Si–2.9% B)

Figure 22 shows a little difference in appearance of the as-brazed and the tested fillet. A large amount of diffusion between the Hastelloy N and the braze alloy is noted. A large amount of deposited material was found on the Hastelloy N (Fig. 22*c*). No compositional changes of the braze were found after test as seen in Fig. 23. Figure 24 shows the electron beam scanning images.

4.8 Braze Alloy BNi-2 (Ni–6.5% Cr–2.5% Fe–4.5% Si–3% B)

Figure 25 shows the as-brazed and the tested fillet. Considerable interaction between the Hastelloy N and the braze alloy is seen. Small deposits were seen on the Hastelloy N. Few compositional changes of the microstructure (Fig. 26) were seen after testing. Some phases very high in chromium are noted as seen in Fig. 27.

5. DISCUSSION

The corrosion resistance of metals to fluoride fuels has been found to vary directly with the "nobility" of the metal, that is, inversely with the magnitude of free energy of formation of fluorides involving the metal. Accordingly, corrosion of multicomponent alloys tends to be manifested by the selective oxidation and removal of the least-noble component. In the case of Hastelloy N, corrosion is selective with respect to chromium. Examples of chemical reactions which can cause this selective removal of chromium are:

1. Impurities in the melt,

$$FeF_2 \ (NiF_2 \text{ or } HF) + Cr \rightleftharpoons CrF_2 + Fe \ .$$

2. Dissolution of oxide films from the metal surface,

$$2Fe^{3+} \ (\text{or } Ni^{2+}) + 3Cr \rightleftharpoons 2Fe + 3Cr^{2+} \ .$$

3. Constituents in the fuel,

$$Cr + 2UF_4 \rightleftharpoons 2UF_3 + CrF_2 \ .$$

However, conditions could exist whereby soluble impurities in the salt could be reduced, resulting in deposition on the metal surface.

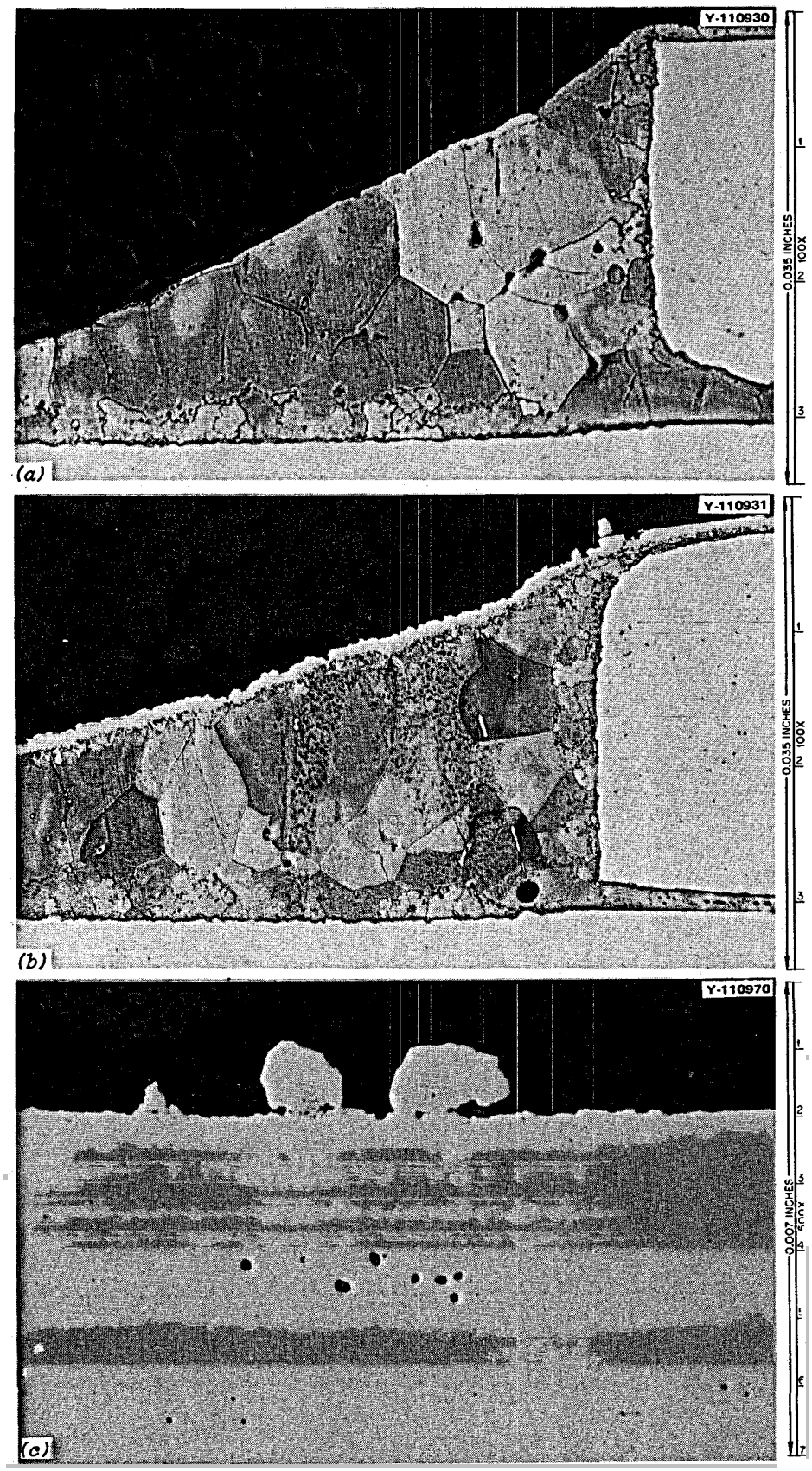

Fig. 19. Braze-alloy BCu (100% Cu) Hastelloy N. As-polished. 100×. (*a*) As-brazed; (*b*) exposed to $NaBF_4$–8 mole % NaF for 4987 hr at 610°C; (*c*) deposit on Hastelloy N after test.

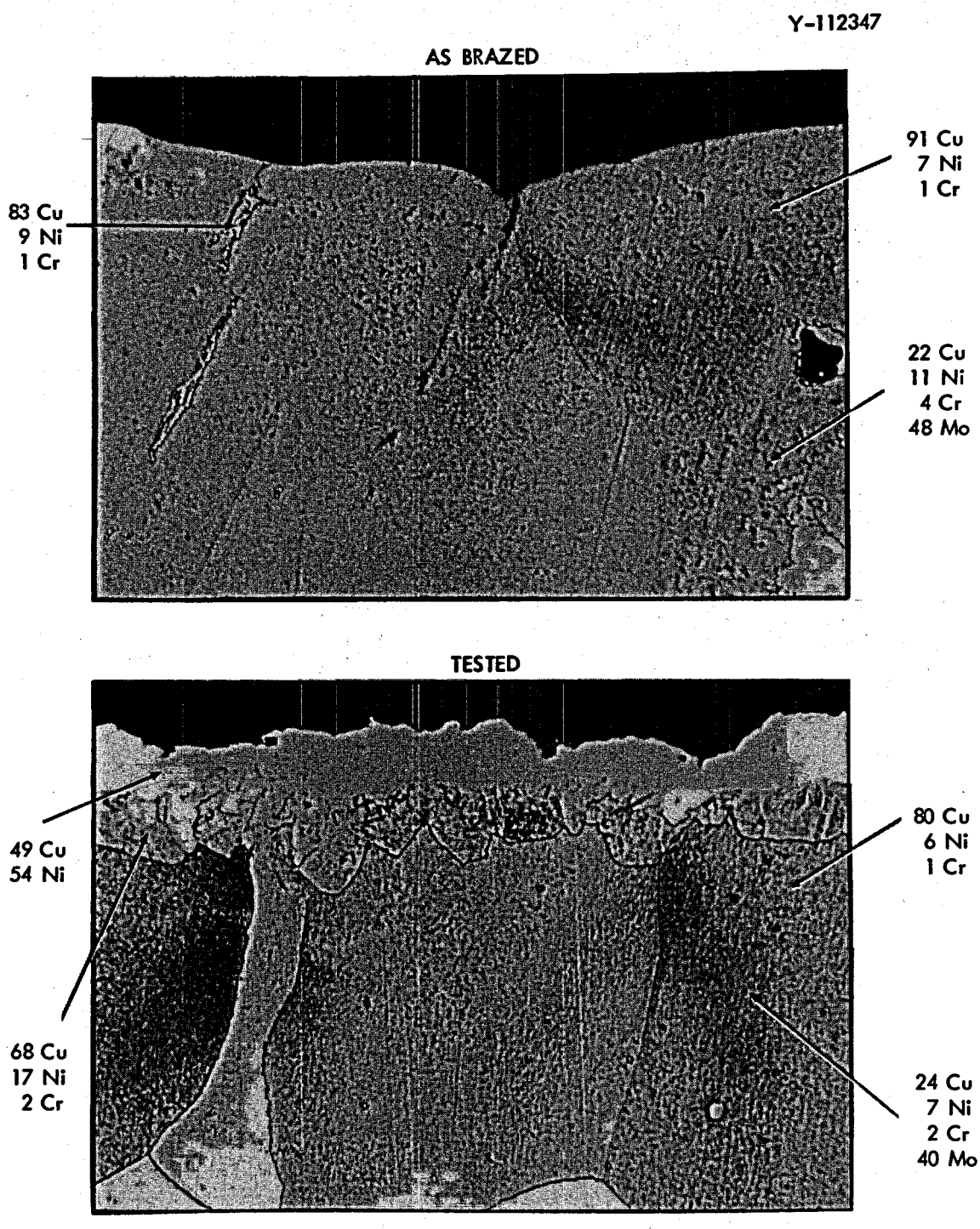

Fig. 20. Microstructural analysis of BCu (100% Cu) braze fillet. Top – as-brazed; bottom – exposed to $NaBF_4$–8 mole % NaF for 4987 hr at 610°C.

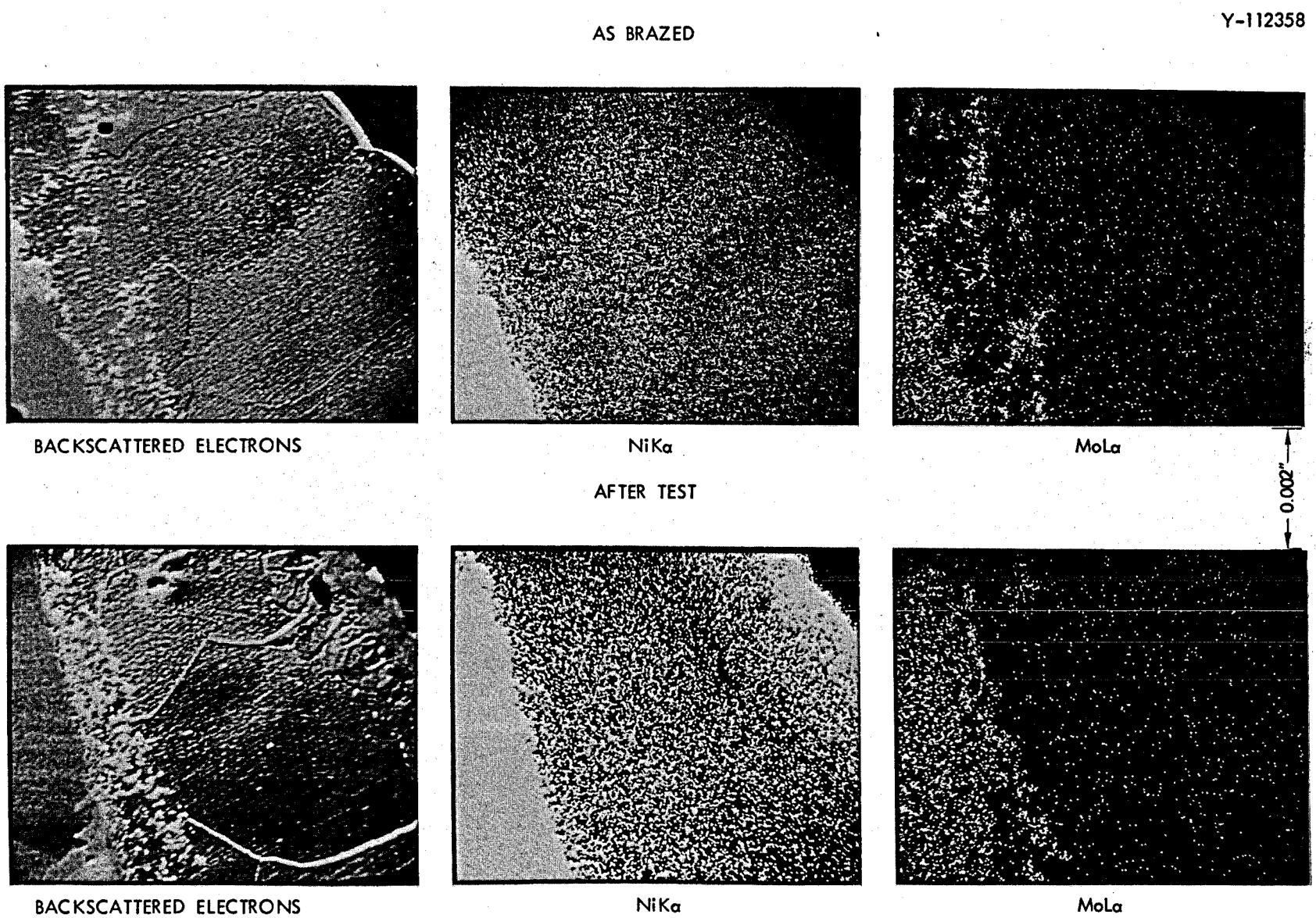

Fig. 21. Electron-beam scanning images of BCu (100% Cu) braze fillet. Top – as-brazed; bottom – exposed to $NaBF_4$–8 mole % NaF for 4987 hr at 610°C.

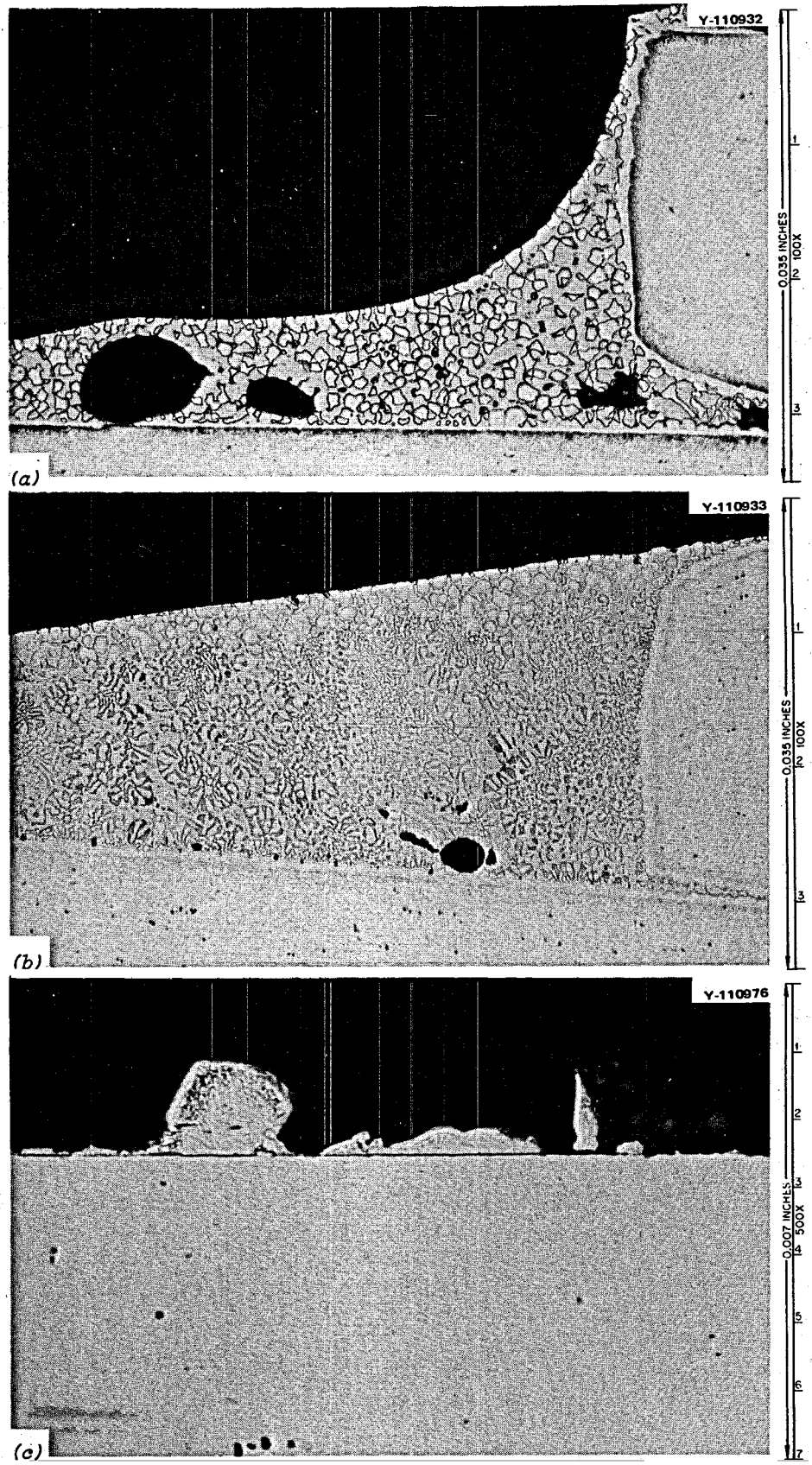

Fig. 22. Braze alloy BNi-2 (Ni–7.0% Cr–4.5% Si–3.5% Fe–2.9% B) Hastelloy N. As-polished. 100X. (*a*) As-brazed; (*b*) exposed to $NaBF_4$–8 mole % NaF for 4987 hr at 610°C; (*c*) deposit on Hastelloy N after test.

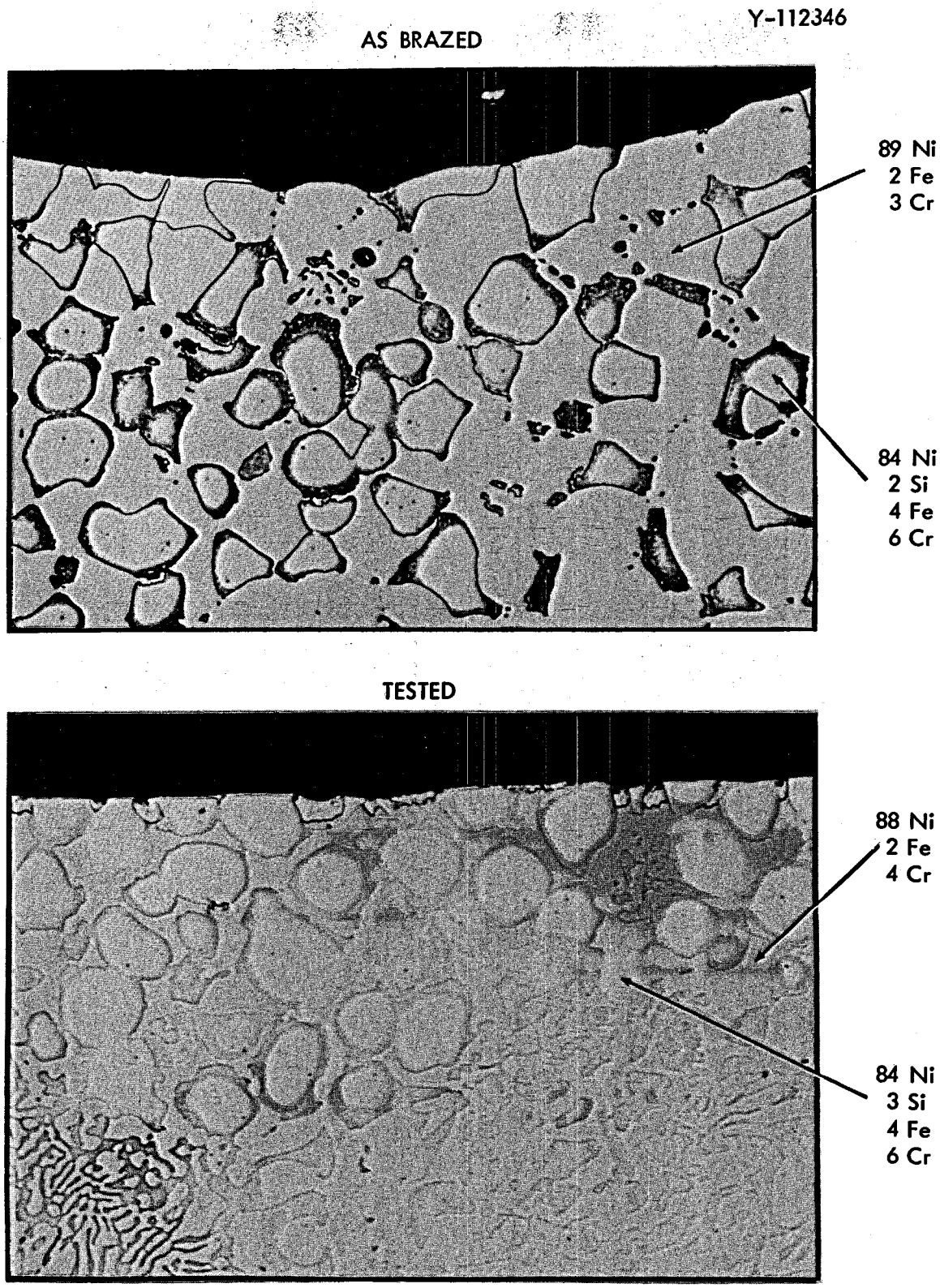

Fig. 23. Microstructural analysis of BNi-2 (Ni–7.0% Cr–4.5% Si–3.5% Fe–2.9% B) braze fillet. Top – as-brazed; bottom – exposed to $NaBF_4$–8 mole % NaF for 4987 hr at 610°C.

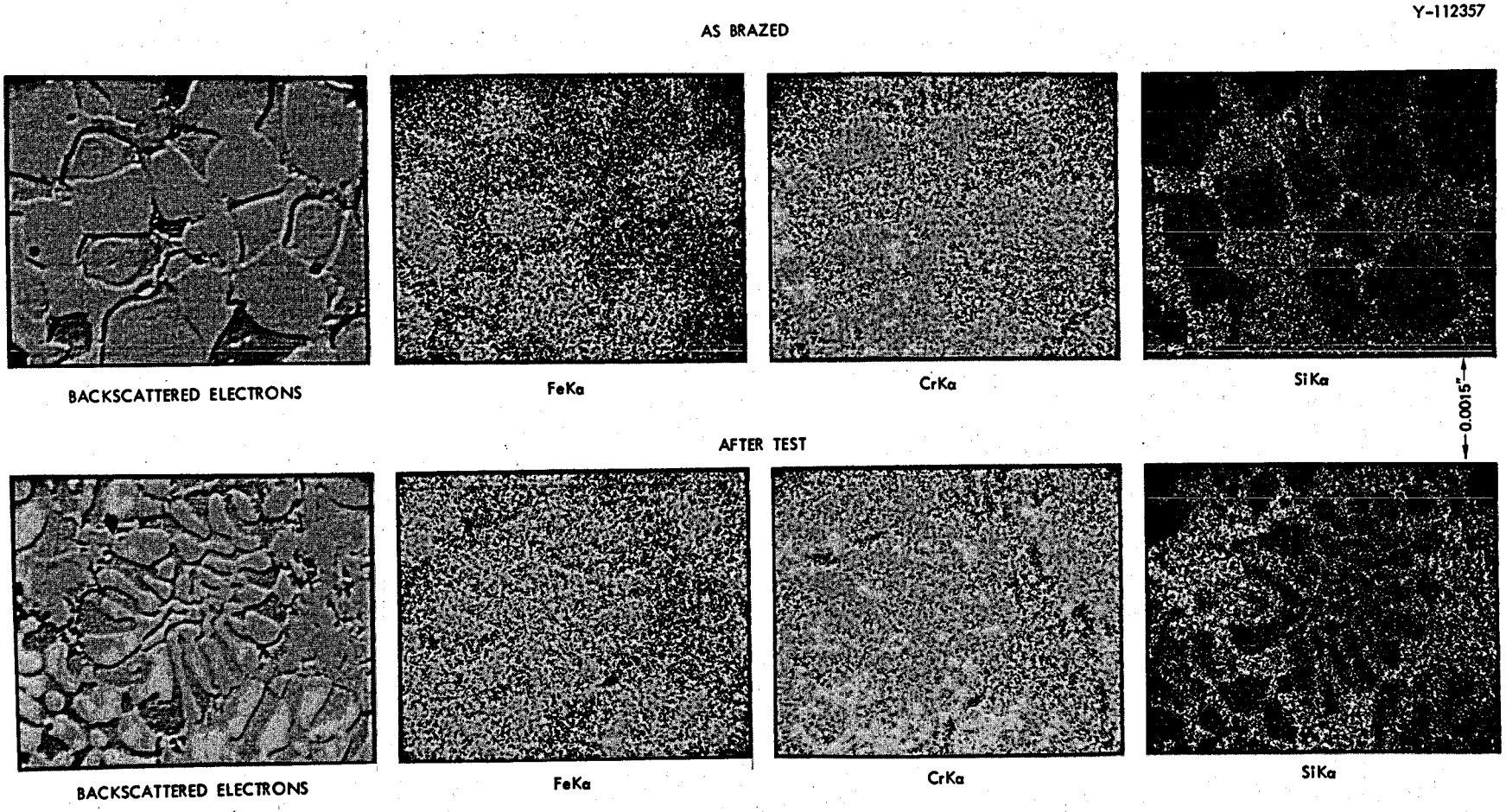

Fig. 24. Electron-beam scanning images of BNi-2 (Ni–7.0% Cr–4.5% Si–3.5% Fe–2.9% B) braze fillet. Top – as-brazed; bottom – exposed to $NaBF_4$–8 mole % NaF for 4987 hr at 610°C.

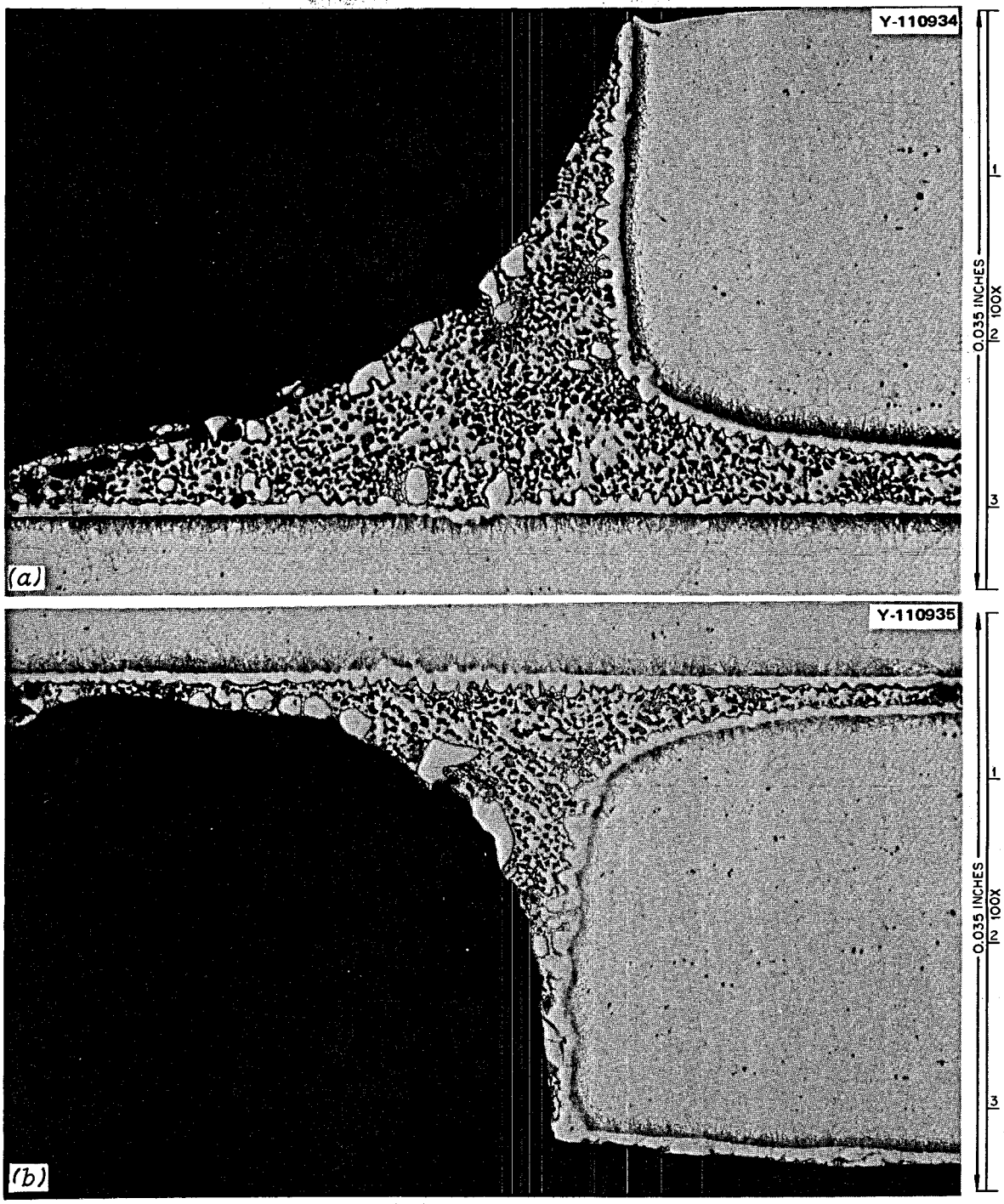

Fig. 25. Braze alloy BNi-2 (Ni–6.5% Cr–4.5% Si–3.0% B–2.5% Fe) Hastelloy N. As-polished. 100×. (*a*) As-brazed; (*b*) exposed to $NaBF_4$–8 mole % NaF for 4987 hr at 610°C.

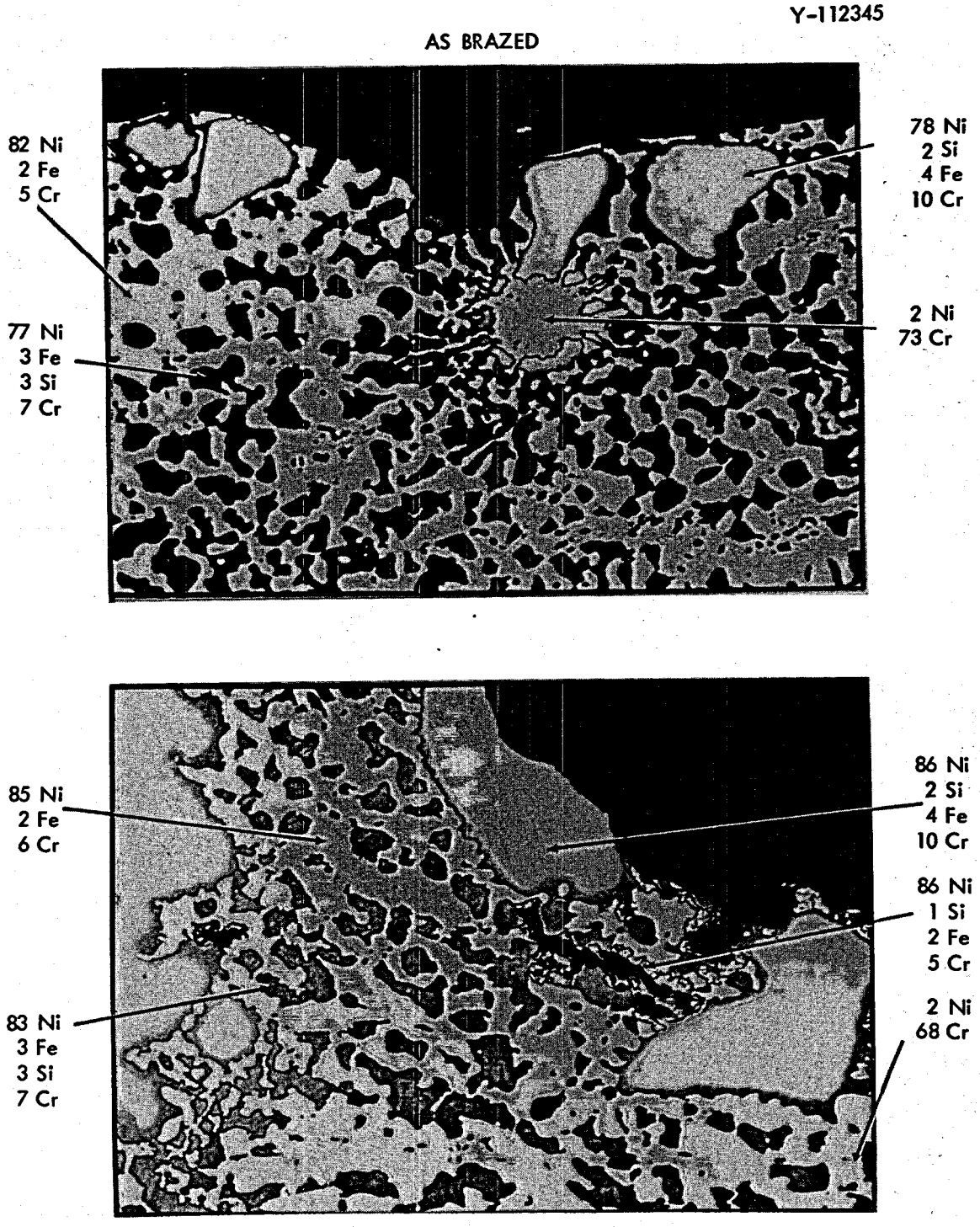

Fig. 26. Microstructural analysis of BNi-2 (Ni–6.5% Cr–4.5% Si–3.0% B–2.5% Fe) braze fillet. Top – as-brazed; bottom – exposed to $NaBF_4$–8 mole % NaF for 4987 hr at 610°C.

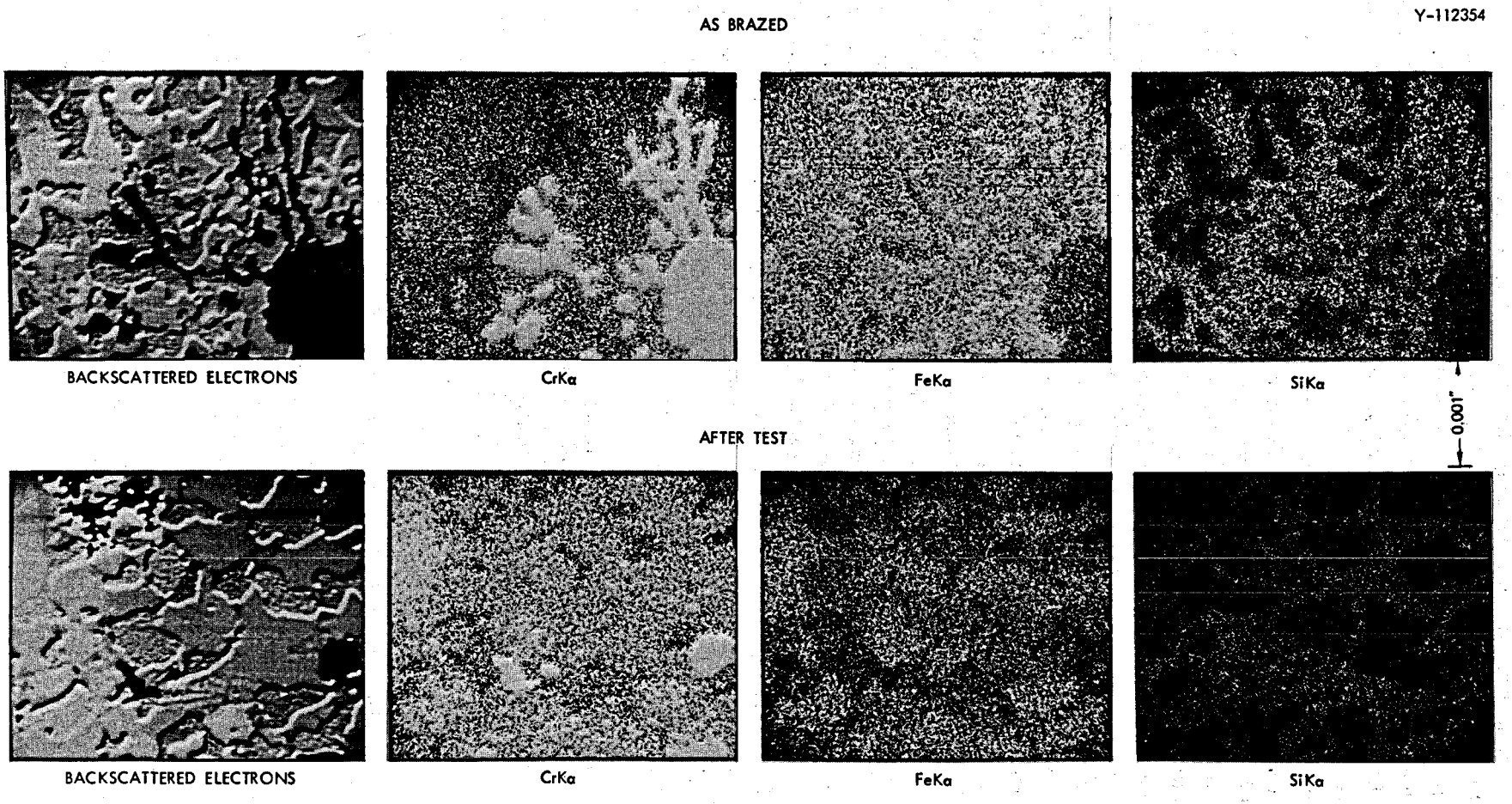

Fig. 27. Electron-beam scanning images of BNi-2 (Ni–0.5% Cr–4.5% Si–3.0% B–2.5% Fe) braze fillet. Top – as-brazed; bottom – exposed to $NaBF_4$–8 mole % NaF for 4987 hr at 610°C.

Another consideration in this experiment is the effect of joined dissimilar metals. A potential difference usually exists between two dissimilar metals when they are immersed in a corrosive or conductive solution. If these metals are placed in contact (or otherwise electrically connected), this potential difference produces electron flow between them. Corrosion of the less resistant metal (or alloy) is usually increased, and attack of the more resistant material is decreased, as compared with the behavior of these metals when they are not in contact.

The potential differences between metals under reversible, or noncorroding, conditions form the basis for predicting corrosion tendencies. These potentials can be indicated by taking the absolute differences between the free energies of formation of the corrosion products. Table 11 gives the free energy of formation of various fluorides at 600°C and includes metals present in the Hastelloy N or in the braze alloy. No series of potentials or free energies exist for alloys in molten salts like that found for alloys in seawater.

The potential generated by a galvanic cell consisting of dissimilar metals can change with time. As corrosion progresses, reaction products or corrosion products may accumulate at either the anode or cathode or both and reduce the speed at which corrosion proceeds. The polarizability of one of the metals of the galvanic couple also may affect the galvanic action; thus it is quite difficult to predict the galvanic behavior, and experiments necessarily must be conducted.

We will discuss the nobility of the braze alloy as compared with the Hastelloy N, considering the constituents of each and the free energy of formation of the various fluorides strictly on a theoretical thermodynamic basis with no regard for kinetics. Braze alloys 1, 7, and 8 contain chromium, silicon, and boron, which form rather stable fluorides. Thus we assume that the braze alloy is probably less noble than Hastelloy N. Braze alloys 2 and 5 also contain sufficient amounts of silicon and boron, so again these alloys are probably less noble than the Hastelloy N. Because of the presence of the relatively noble gold, silver, and copper, braze alloys 3, 4, and 6 should be more noble than the Hastelloy N. If there is corrosion, braze alloys 1, 2, 5, 7, 9 should be selectively attacked with respect to Hastelloy N, and Hastelloy N should be attacked relative to braze alloys 3, 4, and 6. We point out that all the brazed specimens have Hastelloy N in common. Thus, those brazes less noble than Hastelloy N should corrode more than the brazes more noble than Hastelloy N if they are in the same system. Therefore, again emphasizing that there is no consideration

Table 11. Relative thermodynamic stabilities of fluoride compounds formed by elements employed as alloying additions at 600°C[a]

Most stable fluoride compound	Standard free energy of formation per gram atom of fluorine (kcal per gram-atom of F)
BF_3	−87
SiF_4	−85
CrF_2	−76
FeF_2	−69
NiF_2	−62
MoF_6	−58
CuF_2	−50
PF_3	−50
AgF	−38
CF_4	−32
AuF_3	−19

[a]A. Glassner, *The Thermochemical Properties of the Oxides, Fluorides, and Chlorides to 2500°K*, ANL-5750 (1957).

for kinetics, we would predict the following order of corrosion resistance based on alloy composition and free energy of formation of the fluorides:

Braze alloy	No.	
BNi-7	1	Least corrosion resistant
BNi-2	7	
BNi-2	9	
BNi-3	2	
BNi-4	5	
BAu-4	3	
BAg-8	4	
BCu	6	Most corrosion resistant

Brackets indicate alloys in the same order

Since the final weight-change results of this test showed deposition and since deposition is often a function of nucleation sites and times, it is quite difficult to quantify weight-gain data and make comparisons between specimens on weight-gain data. However, since there were two time periods when the oxidizing conditions of the salt were such that some material was lost from the alloy, we decided that these points were sufficient for an experimental comparison of corrosion resistance.

During both time periods when some material was lost from the specimens (Table 9), the BNi-3 braze alloy (No. 2) lost the most weight while the BAg-8 (No. 4) and BCu (No. 6) braze alloys showed the most corrosion resistance. Thus, on the basis of these two time periods when oxidation was greatest the following list is given in the order of increasing corrosion resistance as determined from our experiment:

Braze alloy	No.	
BNi-3	2	Least corrosion resistant
BNi-7	1	
BAu-4	3	
BNi-2	7	
BNi-2	9	
BNi-4	5	
BAg-8	4	
BCu	6	Most corrosion resistant

Brackets indicate alloys in the same order

The experimental results agree with our theoretical listing in the case of specimens 4 and 6; however, specimens 3 and 2 were not as resistant as expected. No explanation can be given for the behavior of specimen 3 (the Au-Ni braze) since, in the past, it has proven to be quite resistant in molten salts. Specimens 1, 2, 7, and 9 all contain from 10 to 14% Si, B, and Cr, all of which form stable fluorides, so their position in the table is not surprising. It is also gratifying that the BNi-2 brazes from different manufacturers acted about the same. Specimen 5 has smaller amounts of these elements and improved corrosion resistance. Thus consideration of the free energy of formation of corrosion products by the alloying elements in the braze can be used to predict the corrosion resistance of most of the brazes. Another area to consider is the nobility of the braze as compared with the Hastelloy N. In most cases it would be preferable to have a braze alloy more noble than the Hastelloy N since there is a much smaller quantity of braze alloy that could be attacked. All in all, none of the corrosion rates are excessive.

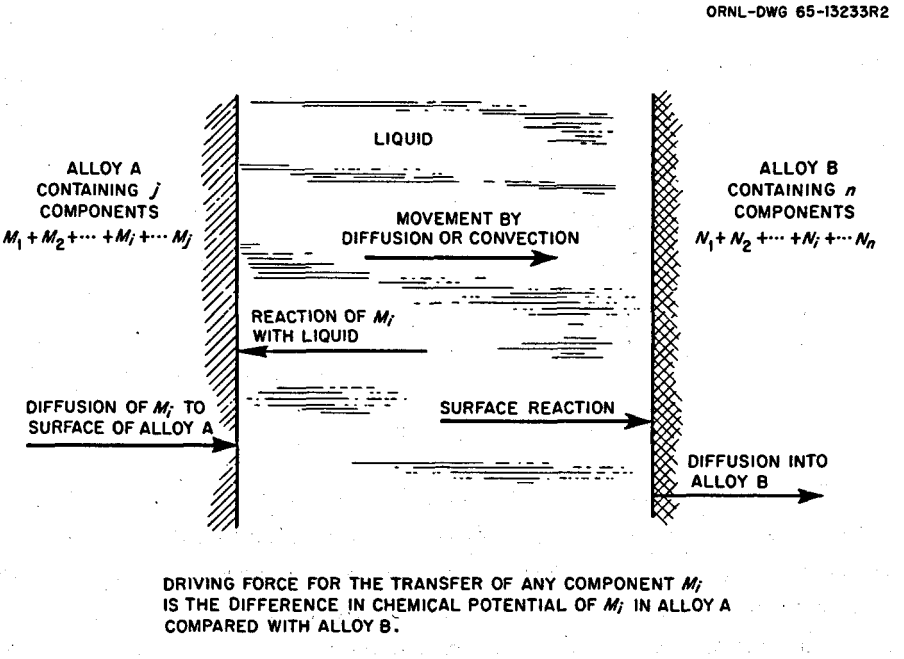

Fig. 28. Dissimilar-alloy mass transfer.

It is also interesting to note that specimens 4 and 6 had deposits on the braze fillets. These deposits appear to be due to activity-gradient mass transfer. Mass transfer of this type only requires the presence of different alloys in the same fluid. Figure 28 shows a schematic of this process. The sequence of events in dissimilar alloy mass transfer involves removal of material from one metal and deposition on a second metal, that is, movement from a region of high activity to one of low activity. Examples of dissimilar metal interactions have been seen in niobium and type 316 stainless steel systems exposed simultaneously to sodium-potassium alloy,[23] other liquid metal-alloy systems,[24] and in a Hastelloy N–Haynes alloy No. 25–molten sodium fluoroborate mixture system.[25] In our case, assuming the products to be deposited consisted mainly of the constituents of Hastelloy N (which is mostly nickel), the only materials in the system that do not contain nickel are the braze alloys of specimens 4 and 6. Thus the deposits of nickel (which diffused into the braze alloy) were a result of transfer to an area of low activity.

The fact that very little salt chemistry change was seen also was evidence that we had activity-gradient transfer between the braze alloy and the Hastelloy N with the salt only acting as a carrier. However, the weight gains are evidence that some material is transferred from the salt or the pot to the alloys. Calculations show that only 50 ppm of material needed to be removed from the salt or pot to equal the measured weight gains.

The micrographs substantiate the small measured weight gains and show no real evidence of attack by the fluoroborate mixture. Of most interest is the interaction between the braze material and the Hastelloy N in certain cases. The nickel-base braze alloys, with the exception of specimen No. 1 which differed from the others since it contained 10% phosphorus, showed areas of diffusion between the braze alloy and the

23. J. R. DiStefano, *Mass Transfer Effects on Some Refractory Metal-Alkali Metal Stainless Steel Systems,* ORNL-4028 (November 1966).

24. J. H. DeVan, *Compatibility of Structural Materials with Boiling Potassium,* ORNL-TM-1361 (April 1966).

25. J. W. Koger and A. P. Litman, *Mass Transfer Between Hastelloy N and Haynes Alloy No. 25 in a Molten Sodium Fluoroborate Mixture,* ORNL-TM-3488 (October 1971).

Hastelloy N. No interaction was seen between the gold-, silver-, or copper-based braze alloy and the Hastelloy N. In specimen No. 1, dendrites of composition Ni–15% Cr–1% P extended from the Hastelloy N into the braze alloy. The International Nickel Company[26] recommends that brazing alloys containing phosphorus never be used with any nickel alloys because of the possibility of formation of a phosphide of nickel at the bond. If impact or bending then occurs, failure would be imminent. However, in our case, according to the electron beam scanning images the phosphorus seems to be fairly well dispersed.

The Stellite Division of Cabot Corporation[27] warns against using brazing alloys that contain copper with Hastelloy alloys. They say that the infusion of copper into grain boundaries can affect both the corrosion resistance and the mechanical properties. We saw no evidence, in either of our copper-containing brazes, of copper interaction with the Hastelloy N. We did see mixing of the Hastelloy N constituents with the copper. Copper does alloy quite readily with nickel but will generally not flow too far before it has picked up enough nickel to raise its liquidus and reduce its fluidity.

Because of strength and oxidation characteristics BAg-8 alloy No. 4 (Ag–28% Cu) is generally not used at temperatures over 400°C, and the copper braze alloy should probably not be used at temperatures above 500°C.[26] We observed no problem with these alloys at 610°C in a molten fluoride salt.

6. CONCLUSIONS

1. On the basis of corrosion resistance, all the braze alloys tested under our conditions are compatible with $NaBF_4$–8 mole % NaF at 610°C. The Ag–28% Cu and 100% Cu braze alloys were the most resistant.
2. Prediction of corrosion resistance on the basis of free energy of formation data is reasonable.
3. Nickel transferred to non-nickel-containing braze alloys through an activity-gradient mass transfer mechanism.
4. Some deposits were noted on the Hastelloy N base material.
5. Diffusion between the Hastelloy N and the braze alloy occurred only with those braze alloys whose composition was near that of Hastelloy N.

---

26. Huntington Alloy Products Division of the International Nickel Co., Inc., *Joining the Huntington Alloys,* Technical Bulletin T-2, 1967.
27. Stellite Division of Cabot Corporation, *Fabrication of Hastelloy Alloys,* F-30, 126F, 1970.

INTERNAL DISTRIBUTION

(79 copies)

(3) Central Research Library
ORNL – Y-12 Technical Library
Document Reference Section
(10) Laboratory Records Department
Laboratory Records, ORNL RC
ORNL Patent Office
G. M. Adamson, Jr.
C. F. Baes
C. E. Bamberger
S. E. Beall
E. G. Bohlmann
R. B. Briggs
S. Cantor
E. L. Compere
W. H. Cook
F. L. Culler
J. E. Cunningham
J. M. Dale
J. H. DeVan
J. R. DiStefano
J. R. Engel
D. E. Ferguson
J. H. Frye, Jr.
L. O. Gilpatrick
W. R. Grimes
A. G. Grindell
W. O. Harms
P. N. Haubenreich
(3) M. R. Hill
W. R. Huntley
H. Inouye
P. R. Kasten
(5) J. W. Koger
E. J. Lawrence
A. L. Lotts
T. S. Lundy
R. N. Lyon
H. G. MacPherson
R. E. MacPherson
W. R. Martin
R. W. McClung
H. E. McCoy
C. J. McHargue
H. A. McLain
B. McNabb
L. E. McNeese
A. S. Meyer
R. B. Parker
P. Patriarca
A. M. Perry
M. W. Rosenthal
H. C. Savage
J. L. Scott
J. H. Shaffer
G. M. Slaughter
G. P. Smith
R. A. Strehlow
R. E. Thoma
D. B. Trauger
A. M. Weinberg
J. R. Weir
J. C. White
L. V. Wilson

EXTERNAL DISTRIBUTION

(24 copies)

BABCOCK & WILCOX COMPANY, P. O. Box 1260, Lynchburg, VA 24505
B. Mong

BLACK AND VEATCH, P. O. Box 8405, Kansas City, MO 64114
C. B. Deering

BRYON JACKSON PUMP, P. O. Box 2017, Los Angeles, CA 90054
G. C. Clasby

CABOT CORPORATION, STELLITE DIVISION, 1020 Park Ave., Kokomo, IN 46901
T. K. Roche

CONTINENTAL OIL COMPANY, Ponca City, OK 74601
J. A. Acciarri

EBASCO SERVICES, INC., 2 Rector Street, New York, NY 10006
D. R. deBoisblanc
T. A. Flynn

THE INTERNATIONAL NICKEL COMPANY, Huntington, WV 25720
J. M. Martin

UNION CARBIDE CORPORATION, CARBON PRODUCTS DIVISION, 12900 Snow Road, Parma, OH 44130
R. M. Bushong

USAEC, DIVISION OF REACTOR DEVELOPMENT AND TECHNOLOGY, Washington, DC 20545
David Elias
J. E. Fox
Norton Haberman
C. E. Johnson
T. C. Reuther
S. Rosen
Milton Shaw
J. M. Simmons

USAEC, DIVISION OF REGULATIONS, Washington, DC 20545
A. Giambusso

USAEC, RDT SITE REPRESENTATIVES, Oak Ridge National Laboratory, P. O. Box X, Oak Ridge, TN 37830
D. F. Cope
Kermit Laughon
C. L. Matthews

USAEC, OAK RIDGE OPERATIONS, P. O. Box E, Oak Ridge, TN 37830
Research and Technical Support Division

USAEC, TECHNICAL INFORMATION CENTER, P. O. Box 62, Oak Ridge, TN 37830
(2)